REVISED RESPONSE TO REQUEST FOR ADDITIONAL INFORMATION

APR1400 Design Certification

Korea Electric Power Corporation / Korea Hydro & Nuclear Power Co., LTD

Docket No. 52-046

RAI No.:	**252-8299**
SRP Section:	**03.07.02 – Seismic System Analysis**
Application Section:	**3.7.2**
Date of RAI Issue:	**10/19/2015**

Question No. 03.07.02-7

10 CFR 50 Appendix S requires that the safety functions of structures, systems, and components (SSCs) must be assured during and after the vibratory ground motion associated with the safe shutdown earthquake (SSE) ground motion through design, testing, or qualification methods. In accordance with 10 CFR 50 Appendix S, the staff reviews the adequacy of the seismic analysis methods used to demonstrate that SSCs can withstand seismic loads and remain functional. To assist the staff in assessing adequacy of the finite element models used for seismic analysis, the applicant is requested to provide additional information related to the following modeling aspects.

a) Conversion of ANSYS Coarse Model to SASSI

Section 2 in APR1400-E-S-NR-14002-P states that the ANSYS coarse 3-D FEM of NI structures is converted to SASSI for a 3-D SSI analysis of NI structures. However the staff did not find a description of how this conversion was performed. The applicant is requested to describe in the report whether this conversion was performed with the ACS SASSI translator or, if not, describe the conversion process used. This description should include a discussion of how the attachment of the superstructure elements to the basemat elements was implemented and how the ability of the resulting FEM model to translate and rotate in a rigid body mode on the supporting soil was verified.

b) Representation of Floor Loads, Live Loads, and Major Equipment in Dynamic Model

SRP Section 3.7.2.II.3D provides the acceptance criteria regarding the representation of floor loads, live loads, and major equipment in a dynamic model. In addressing these SRP criteria, DCD Section 3.7.2.3.3 includes a description of masses that are assumed to contribute to the inertial forces in the seismic analyses. However, this DCD section did not specify the magnitude of such masses. For example, based on the description in DCD Section 3.7.2.3.3, it could be inferred that 100% of the live load is used in the seismic load case. The staff review finds that Section 3.2.5 and Table 4-7 in APR1400-E-S-NR-14002-P,

for the RCB and AB, respectively, provide additional information on the magnitude of the masses described in DCD Section 3.7.2.3.3. Section 3.2.5 in APR1400-E-S-NR-14002-P states that 25 % of floor live load or 75% of snow load are applied on the roof of the containment which appears to conflict with DCD Section 3.7.2.3.3. Based on these two statements it is not clear to the staff what floor live load has been considered on all floors of the reactor containment building. Therefore the staff request the applicant to clarify in the DCD how the SRP Section criteria regarding floor loads is addressed in the models used for seismic analysis.

c) Shell Elements in Primary Shield Wall

As described in Section 3.2.10 and shown Figure 3-3 in APR1400-E-S-NR-14002-P, shell elements are used to model the shield wall portion of the primary shield wall (PSW) from EL 130' to EL 191.' Given the geometry of the PSW, the use of thick shell elements may be more appropriate for this portion of the PSW. he geometry of the PSW, the use of thick shell elements may be more appropriate for this portion of the PSW. Additionally, based on Figure 3-3, a portion of these walls modeled with shell elements, appears to be not in plane with respect to the plane of each respective wall. Therefore to assist the staff in evaluating the adequacy of the FEM for the PSW, the staff requests the applicant to clarify why the shell element selected for the PSW model is appropriate as opposed to using a thick shell element formulation. Additionally, please describe the modeling approach and the basis of the shell portion of the walls including the location of plates oriented in non-parallel planes.

d) Transitions between Beam and Solid Elements

Staff review of APR1400-E-S-NR-14002-P finds that the nuclear island finite element model includes locations at which beam elements connect with solid elements (e.g. connections between the reactor coolant system model and the containment internal structure model). However, the staff did not did not find a description of how the degree of freedom compatibility is addressed for transitions between beam and solid elements. Therefore the staff requests the applicant to provide such description, including a graphical representation of the transition between beam and solid elements.

e) Poisson's Ratio Used in SSI Analyses

DCD Tables 3.7A-1 and 3.7A-2 show Poisson's ratios in the S1 and S2 soil profiles used for SSI analysis as great as 0.47 and 0.48 respectively. Based on staff experience, use of Poisson's ratio approaching these values may result in numerical instability of the SSI analysis results. Therefore, to assist the staff in evaluating the adequacy of the SSI analysis results based on the aforementioned soil profiles, the staff request the applicant to provide a demonstration (e.g. sensitivity study) that the assumed Poisson's ratio values do not produce numerical instabilities in the SSI results based on these profiles.

Response – (Rev. 2)

a) The ANSYS fine-mesh and coarse-mesh finite element (FE) models for the fixed-base Reactor Containment Building (RCB) and the Auxiliary Building (AB) were first developed and analyzed with the fixed-base condition to (1) generate 1-g lateral static-load response displacements, (2) extract fixed-base dynamic modal properties (natural frequencies and

associated mode shapes and participation factors, and (3) develop fixed-base 5%-damped in-structure response spectra (ISRS) at selected sufficiently representative structure locations. The ANSYS coarse-mesh models were verified against their corresponding ANSYS fine-mesh FE models to ensure that the model properties of the ANSYS coarse-mesh models are dynamically adequate as compared to the ANSYS fine-mesh FE models.

When the ANSYS coarse-mesh models of the RCB and the AB are verified, the two models are combined to create an ANSYS coarse-mesh FE model of the NI structures.

Then, the fixed-base ANSYS coarse-mesh FE model of the NI structures was converted to the fixed-base SASSI structure model using the ACS SASSI model translator. The converted SASSI structure model was checked manually to ensure that the SASSI structure model was appropriately converted from the ANSYS model.

Then, the converted SASSI fixed-base structure model was analyzed for the fixed-base condition to develop fixed-base seismic acceleration response transfer functions and the corresponding 5%-damped ISRS at the same selected representative structure locations as those selected for the ANSYS model. These ISRS results were compared with the corresponding results obtained from the fixed-base ANSYS structure model to verify that the converted fixed-base SASSI structure model produces results which are sufficiently similar to the corresponding results of the fixed-base ANSYS structure model.

The SASSI foundation model which is combined with the SASSI structure model consists of a common basemat structure model, an excavated soil volume model for the structure embedment developed to use the SASSI Direct Method (DM), and a backfill soil model which was treated as a part of the structure model. The SASSI foundation model for the NI structures was so developed and checked manually.

The common basemat for the AB and the RCB was modeled separately by 4-node shell elements for the AB at the bottom surface of concrete foundation (EL. 45’-0”) to specially account more closely for the soil-structure interaction effects, and by 8-node solid elements for the RCB concrete foundation, respectively. To ensure continuity of rotational deformation at the interface of the AB shell elements and the RCB solid elements, a dummy massless ring of shell elements was extended from the outside edge to the inside of the RCB, beneath the solid elements. To simulate the relatively rigid 10-ft basemat between the top (EL. 55’-0”) and the bottom (EL. 45’-0”) surfaces of the concrete foundation for the AB, the AB walls and columns were extended from EL. 55’-0” to EL. 45’-0” with massless rigid beam elements.

The ability of the resulting SASSI FE SSI model to translate and rotate was demonstrated by observing that the resulting seismic response transfer functions are able to translate and rotate as a rigid body on the supporting soil.

Technical report APR1400-E-S-NR-14002-P, Rev. 0, “FEM for SSI Analyses of NI Buildings” will be revised, as indicated in Attachment 1 to this response, to incorporate the procedures described above for development of the ACS SASSI models for the NI structures.

b) In general, in addition to the mass of the tributary structure dead load, additional mass equivalent to 25% of the specified floor live load or 75% of the specified snow load, where applicable; 50 psf, the equivalent of the miscellaneous dead load supported on the floors;

and 10 psf, the equivalent of the attachment load on each face of the walls are included in the calculation of the inertia forces of the model. However, there are some exceptions, for example, 25% of floor live load is not considered in the RCB floors, and the roof material dead load is considered only for the AB roof. The magnitudes of masses on the floors are presented in the following table.

Masses that are considered to contribute to the inertial forces			
Description	Value (psf)	RCB	AB
Misc. dead load (Minor equipment, piping, race ways)	50.00	Applied	Applied
Seismic live load(1) (25% of floor design load 200 psf)	50.00	Not Applied	Applied
Roof snow load (75% of roof design snow load 75 psf)	56.25	Applied	Applied
Roofing material dead load(2)	50.00	Not Applied	Applied
Raised floor dead load(3)	20.00	Not Applied	Applied

(1) Seismic live load is not considered for floors in the RCB.

(2) The roof of the RCB, i.e. containment dome, does not use roofing material.

(3) The raised floor dead load is only applicable for the floor at EL. 156’-0” of the AB.

DCD Tier 2, Subsection 3.7.2.3.3 and technical report APR1400-E-S-NR-14002-P will be revised as indicated in Attachment 2 to this response to incorporate brief descriptions of the masses considered in the seismic analyses.

In the seismic analysis model of the RCB, the slabs at EL. 114’-0”, 136’-6”, and 156’-0” between the secondary shield wall (SSW) and the containment shell (CS) are not modeled in accordance with the decoupling criteria presented in the USNRC SRP 3.7.2. All the masses of those slabs considering the self-weight, 50 psf of the miscellaneous attachment dead load, and the major equipment loads are lumped onto the SSW. The slabs between the SSW and the CS are completely connected to the SSW, and there are a minimum of 2 inches gaps between CS and the slabs. In addition, the supporting beams under the slabs have sliding connection at the CS. Therefore, all the horizontal slab masses would be actually lumped onto the SSW, and part of the vertical slab masses would be actually applied to the CS due to the beam seats at the CS. However, concentration of the vertical slab masses onto the SSW only would not cause much frequency discrepancies because the slab masses are not large in comparison with the SSW and the CS masses. Therefore, the SSW is considered as the main supporting structure for the slabs between the SSW and the CS in the seismic analysis model of the RCB.

To ensure the connection of the slabs at the CS side are consistent with the modeling assumption of the RCB seismic analysis model, the description of sliding connection design at the CS side of the structural steel beams under the slabs between the SSW and the CS will be added to DCD Tier 2, Subsection 3.8A.1.4.3.4.3 as Attachment 1 of revised response to RAI 248-8295, Question 03.08.05-1, Rev. 1.

In general, the slabs that are not modeled in the seismic analysis model of the RCB are used for the movement of person and equipment during the construction or maintenance periods. Therefore, most of the ISRS for those slabs are not required. In the case where the ISRS of the slab is not modeled in the seismic analysis model, an amplified vertical ISRS can be developed from the vertical seismic response motions of the CS and the SSW using a local model for the slab vertical vibration modes. Since the slabs have sliding connections at the CS, the horizontal behavior of the slabs must be quite rigid due to the membrane action.

Except for the slabs between the SSW and the CS described above, all other slabs in the RCB are modeled in the seismic analysis model of the RCB. The figures and the fundamental frequencies of those slabs in the coarse mesh and fine mesh RCB models are presented in Figures 1 through 6 and Table 1. The average mesh sizes of the coarse and fine slab models are approximately 5 ft x 5 ft and 10 ft x 10 ft, respectively. As shown in Table 1, the fundamental frequencies of the fine mesh slab models are higher than 50 Hz. The fundamental frequencies of the coarse mesh slab models are similar to the fine mesh slab models. These results indicate that most of the slabs that are modeled in the seismic analysis model of the RCB are quite rigid, and the mesh size of slabs in coarse mesh model is sufficient to accurately capture the out-of-plane flexibility of the slabs.

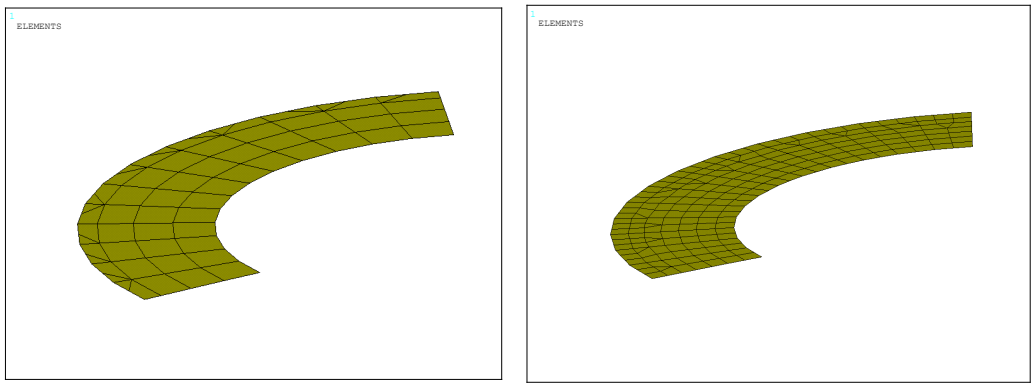

Figure 1. Slab at EL. 100’-0” in Coarse and Fine Mesh RCB Models

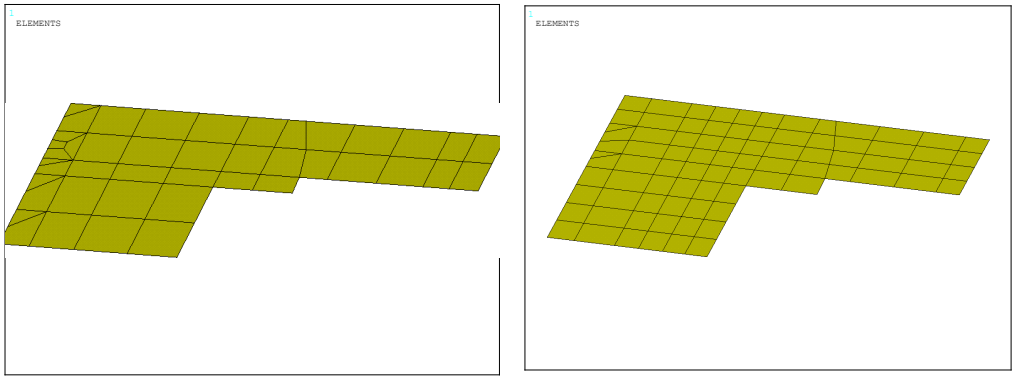

Figure 2. Slab at EL. 111’-0” in Coarse and Fine Mesh RCB Models

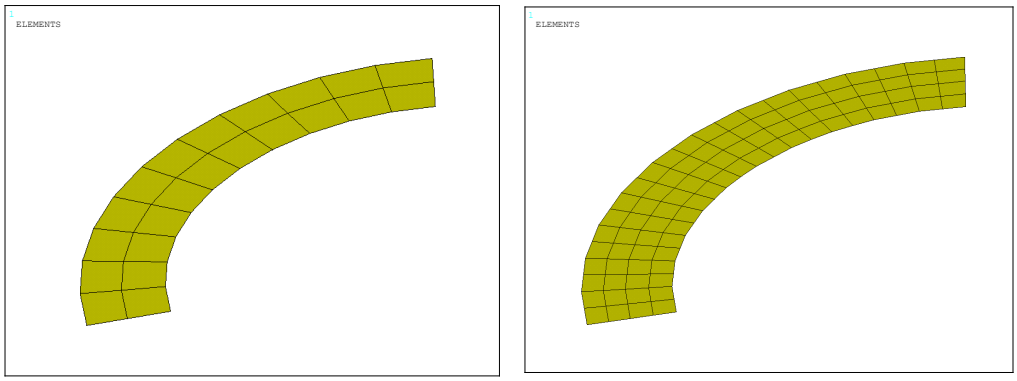

Figure 3. Slab at EL. 114'-0" in Coarse and Fine Mesh RCB Models

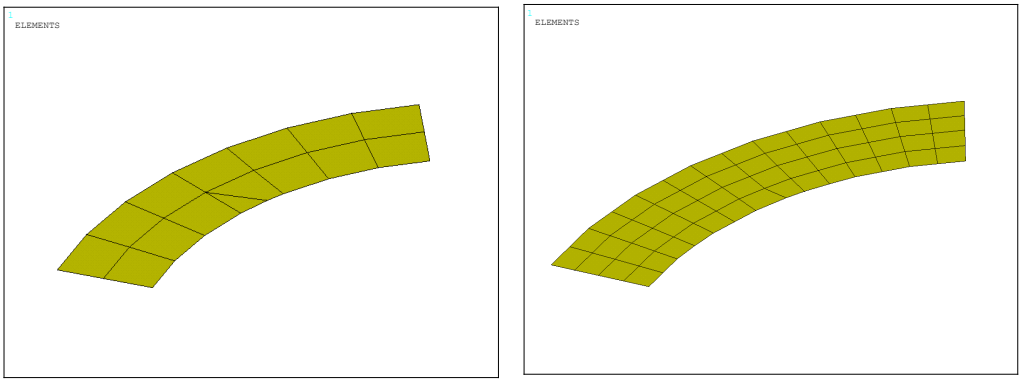

Figure 4. Slab at EL. 125'-0" in Coarse and Fine Mesh RCB Models

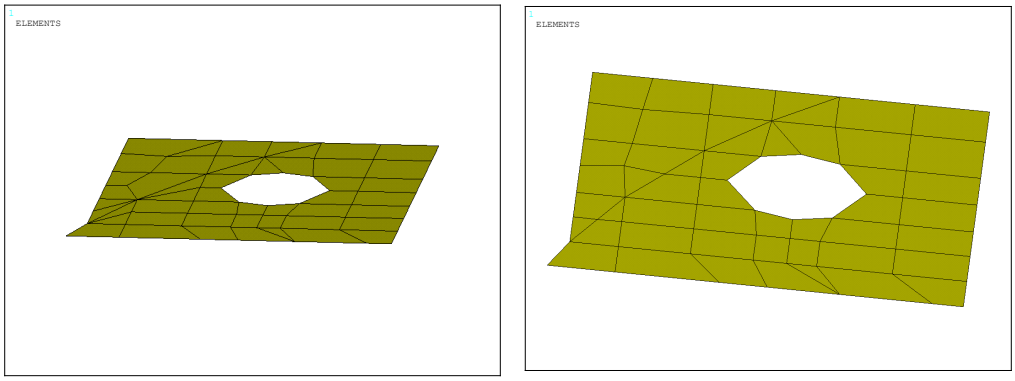

Figure 5. Slab at EL. 133'-3" in Coarse and Fine Mesh RCB Models

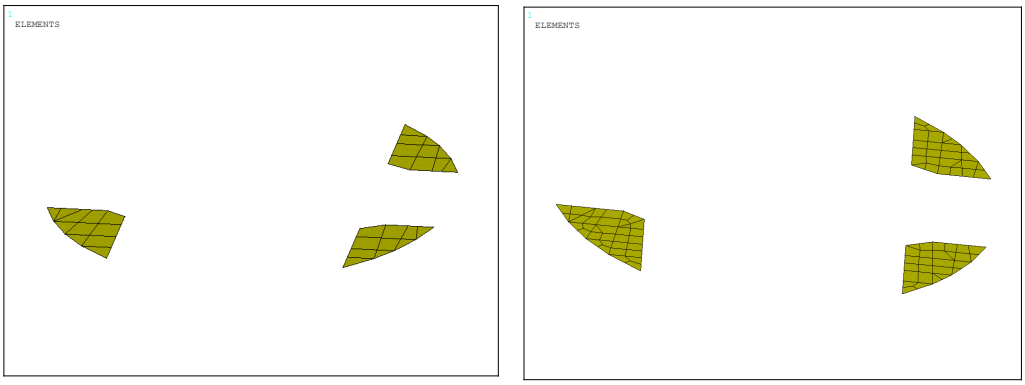

Figure 6. Slab at EL. 156'-0" in Coarse and Fine Mesh RCB Models

Table 1. Fundamental Frequencies of Slabs in Coarse and Fine Mesh RCB Models

Elevation	Fundamental Frequencies (Hz)		Fundamental Frequency Ratio (Coarse / Fine)
	Coarse	Fine	
100'-0"	48.73	50.20	0.97
111'-0"	225.08	229.71	0.98
114'-0"	87.17	93.09	0.94
125'-0"	88.18	94.08	0.94
133'-3"	322.59	323.56	1.00
156'-0"	265.83	275.84	0.96

Since the slabs in the RCB are not large, and the increase of the weight due to the addition of the seismic live load 50 psf (total 1,650 kips) is not great compared to the existing weight of the internal structure walls and slabs (total 183,000 kips), the effect of the seismic live load on the seismic responses of the RCB is expected to be very small.

To evaluate the effect of seismic live load which is not considered in the RCB, a study is performed using the ANSYS coarse mesh model of the RCB. The transient time history analyses are performed with the fixed-base condition using two ANSYS models. One is the original ANSYS coarse mesh model of the RCB, and the other is modified model considering the seismic live load of all slabs in the RCB, whether the slabs are modeled or not. For the slabs which are not modeled, the masses equivalent to the seismic live loads which are applied to the slabs are added to the SSW of the modified model. For the slabs in the model, the lumped masses equivalent to the seismic live loads are added to the nodes of the slabs in the modified model. The CSDRS input time histories of the APR1400 are used as the input time histories for the transient time history analyses. The analyses are performed for individual directions independently. Then, the ISRS results of the three directions are combined using the square root of the sum of the squares (SRSS) method.

The 4%-damped ISRS of the SSW and the slabs that are modeled in the RCB seismic analysis model are compared between two models as presented in Figures 7 through 15.

Since the SSW supports one end side of most slabs in the RCB, the ISRS comparisons of the walls are conducted for SSW only. The nodes, which were used for enveloping the APR1400 ISRS of the SSW, are identically used to generate the enveloped ISRS for the comparisons. For the ISRS comparisons of the slabs that are modeled in the RCB seismic analysis model, the ISRS of the center nodes in each slab are selected and compared as shown in Figures 10 through 15. As shown in the comparison figures, the variation of ISRS due to the consideration of the seismic live load in the RCB seismic analysis model is negligibly small. Therefore, it can be concluded that the effect of seismic live load on the RCB seismic response is insignificant.

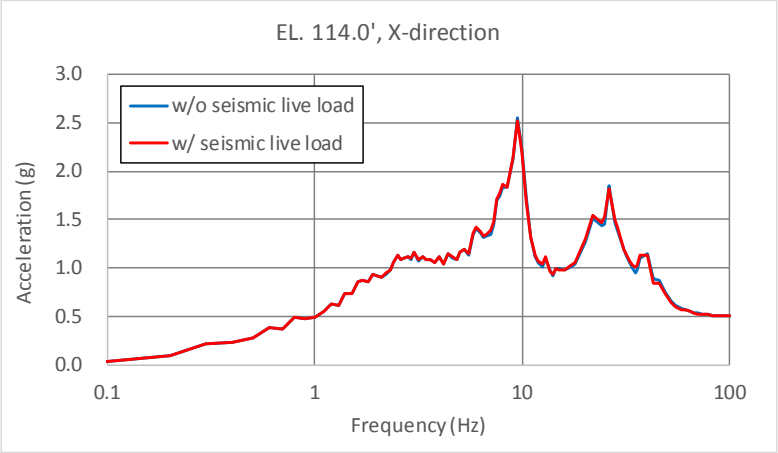

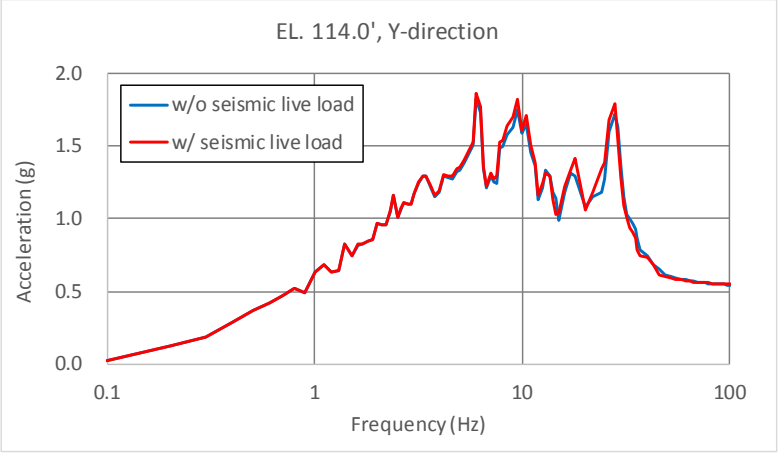

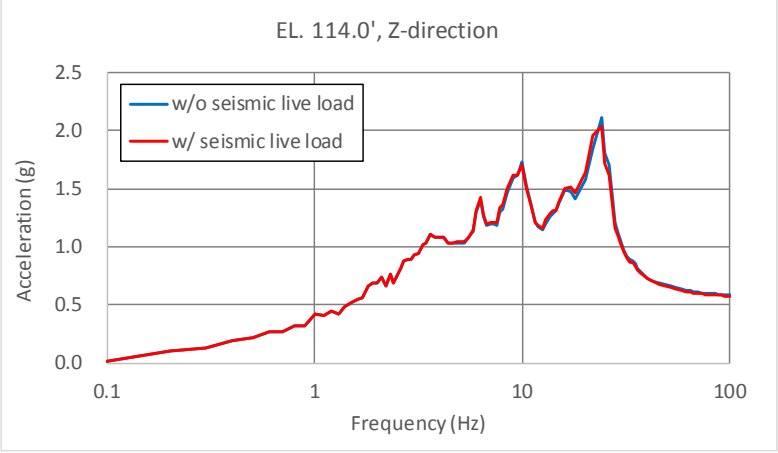

Figure 7. Comparison of SSW ISRS at EL. 114’-0”

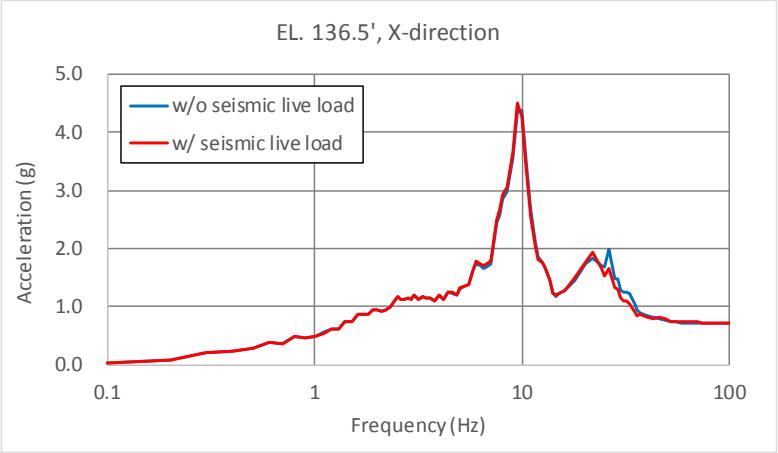

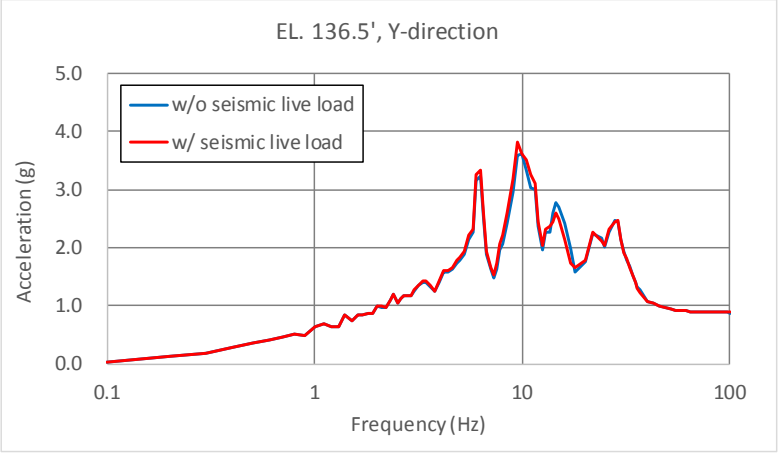

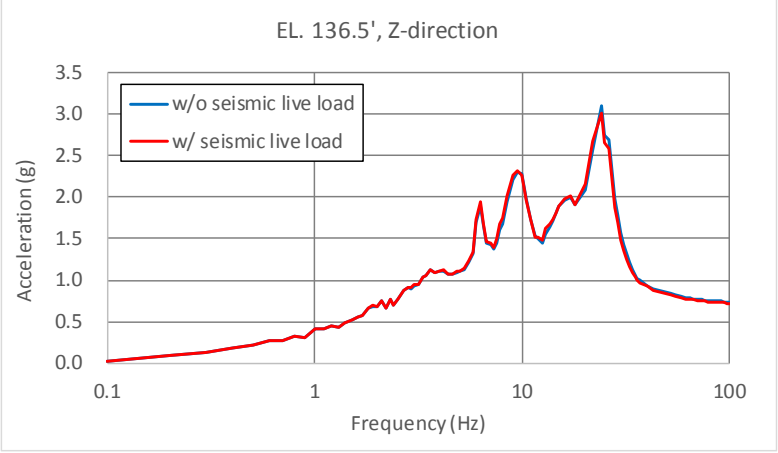

Figure 8. Comparison of SSW ISRS at EL. 136’-6”

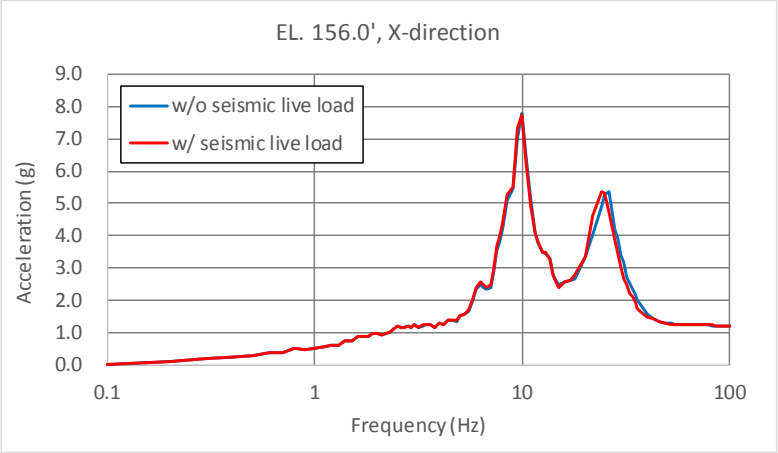

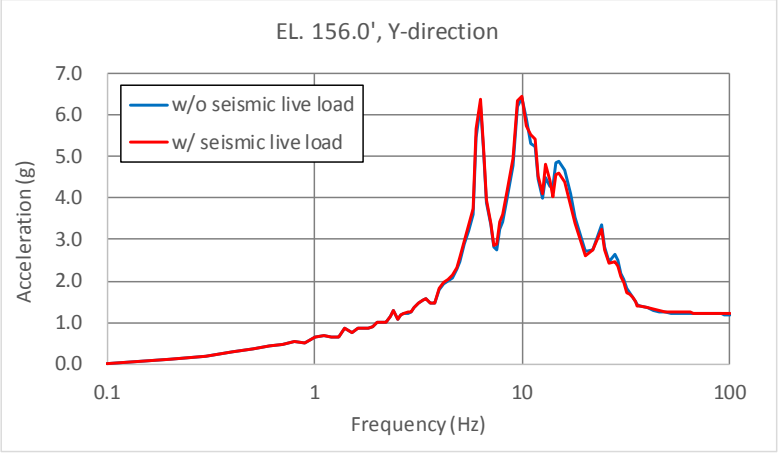

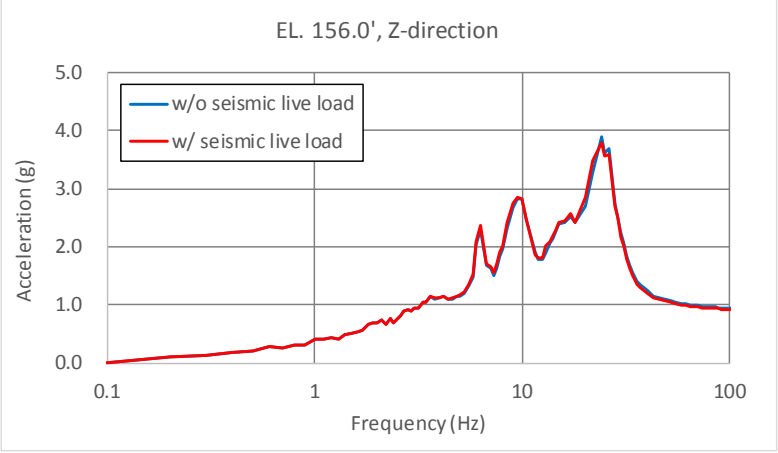

Figure 9. Comparison of SSW ISRS at EL. 156’-0”

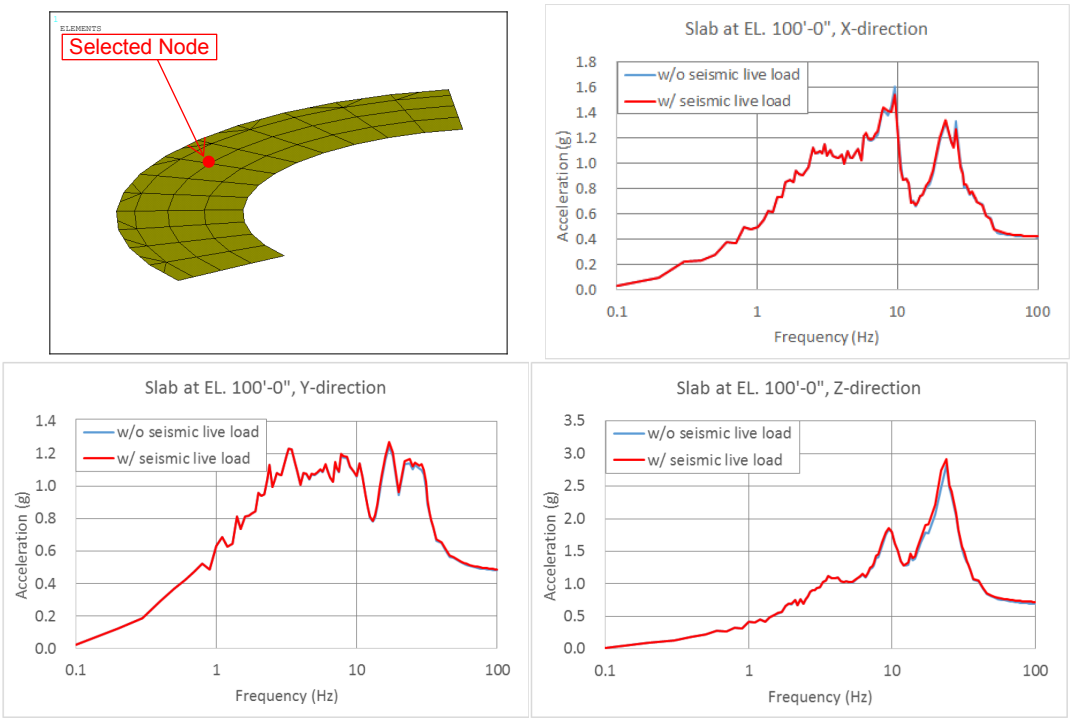

Figure 10. Comparison of Slab ISRS at EL. 100'-0"

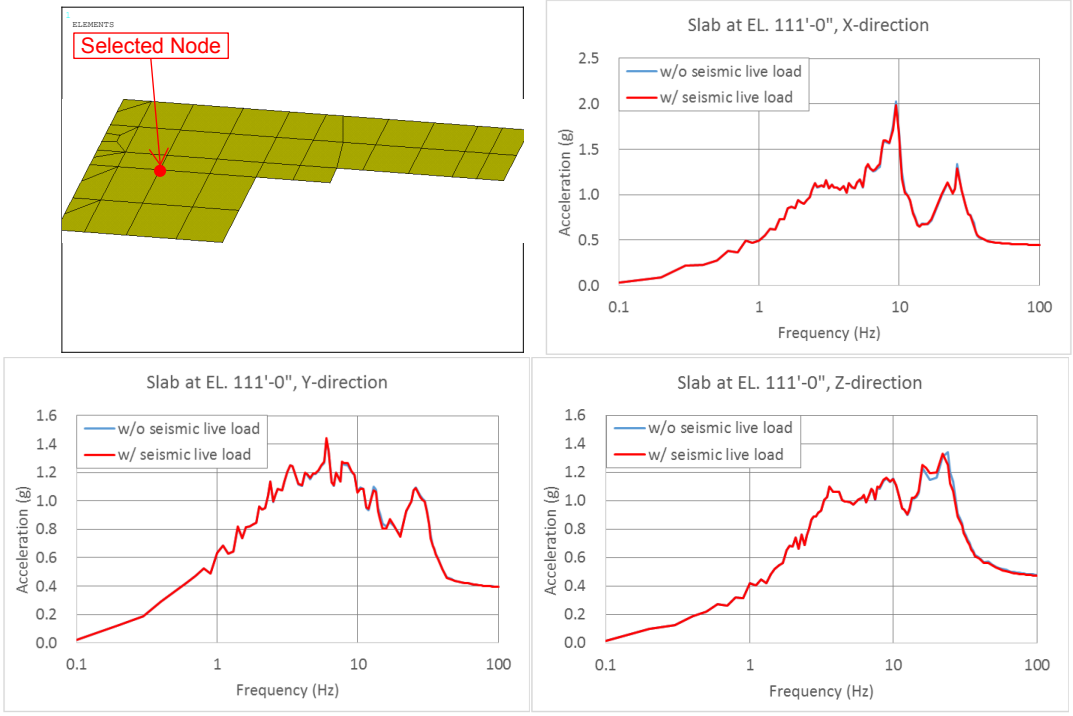

Figure 11. Comparison of Slab ISRS at EL. 111'-0"

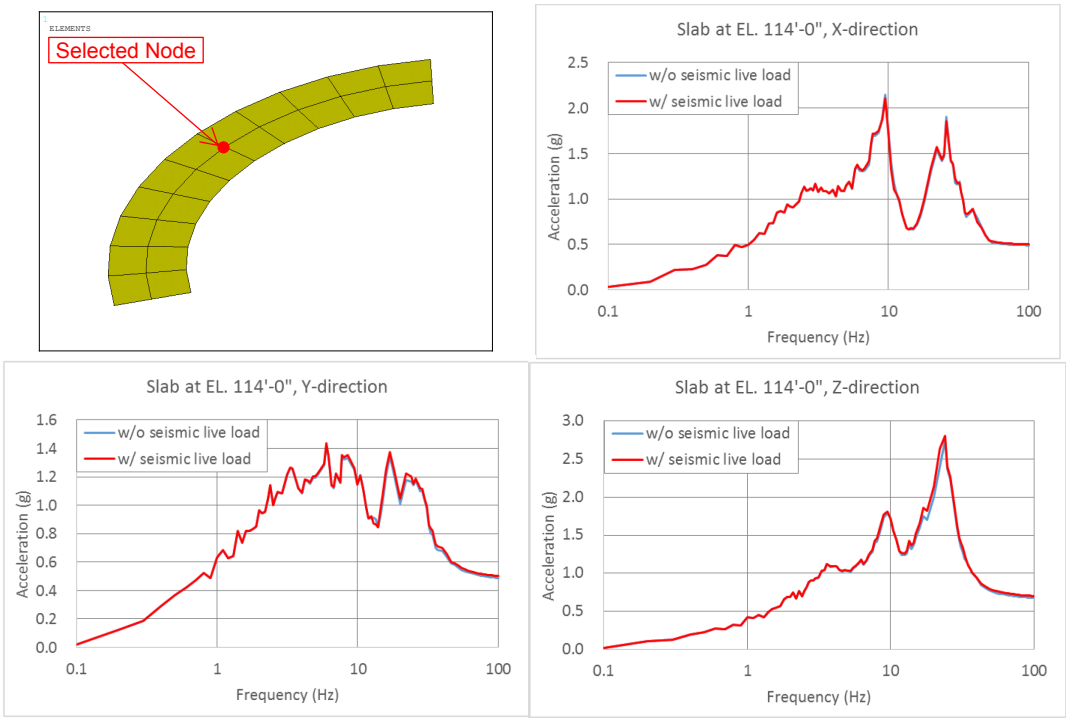

Figure 12. Comparison of Slab ISRS at EL. 114'-0"

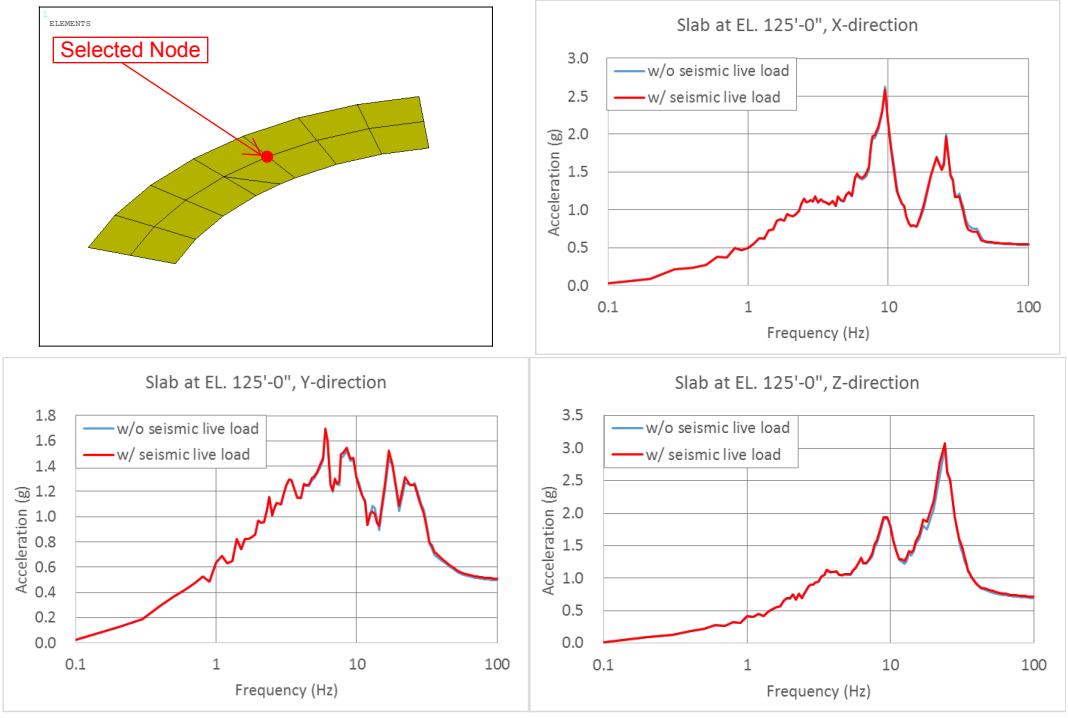

Figure 13. Comparison of Slab ISRS at EL. 125'-0"

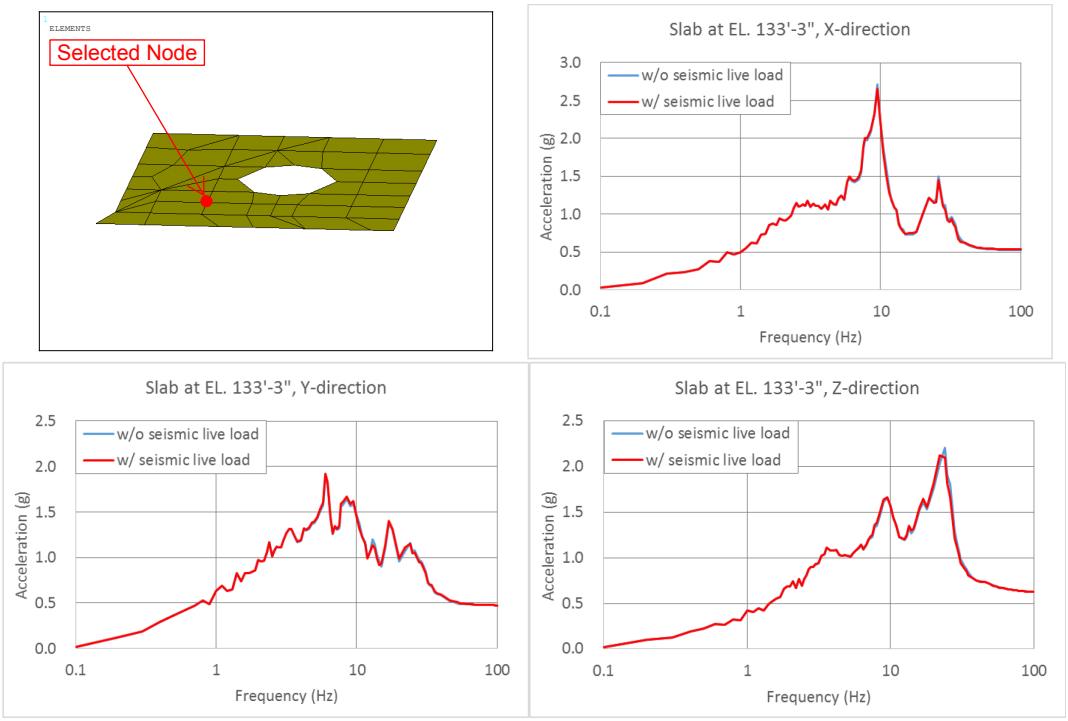

Figure 14. Comparison of Slab ISRS at EL. 133'-3"

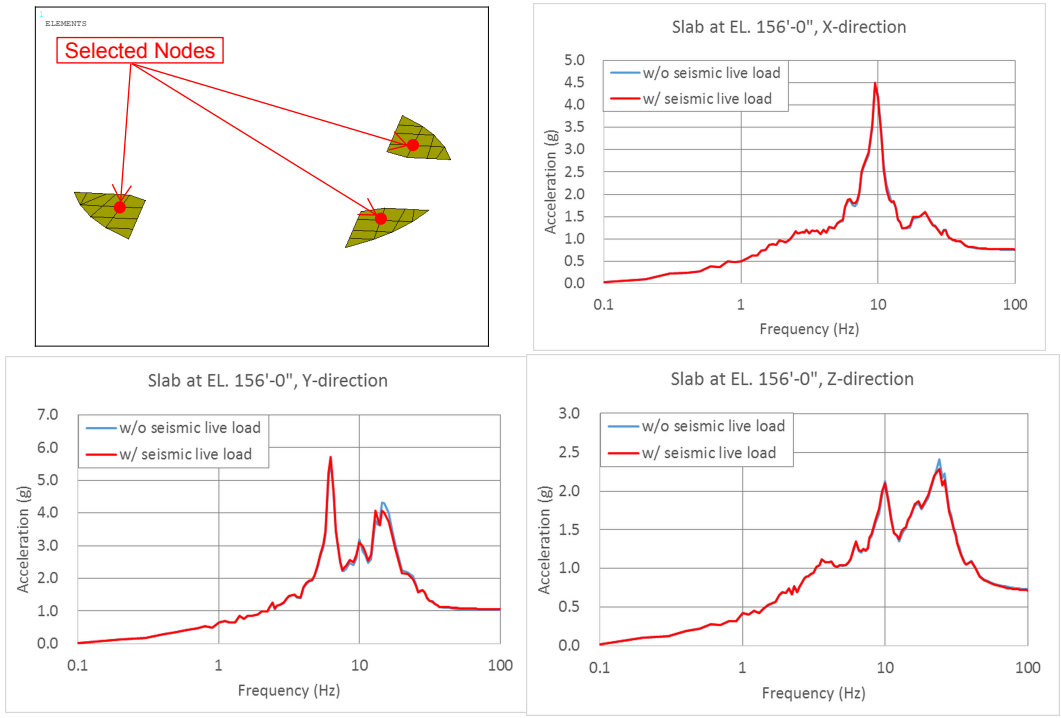

Figure 15. Comparison of Slab ISRS at EL. 156'-0"

c) The original SASSI program was developed in the 1980's and has only the LCCT9 thin shell element, which was adopted from the SAP IV structural analysis program. This same version of the SASSI code was adopted by many company-specific versions of SASSI. ACS SASSI 2.3 also has only the LCCT9 thin shell element. Many versions of SASSI, including ACS SASSI 2.3, do not have thick shell element available for structural modeling. This is the reason why thick shell elements have not been used for modeling the PSW by the ANSYS program.

Use of thick or thin shell elements does not significantly affect the overall structural stiffness since the main stiffness of the shell structures (containment shell, PSW, SSW, etc.) are primarily due to in-plane stiffness.

The thickness and center axis of the PSW section are changed over EL. 147'-9" through EL. 154'-0", as shown in Figure 16. The portion of wall which is not in plane with respect to the plane of respective walls in Figure 3-3 of APR1400-E-S-NR-14002-P was intentionally modeled to represent the contour of the PSW.

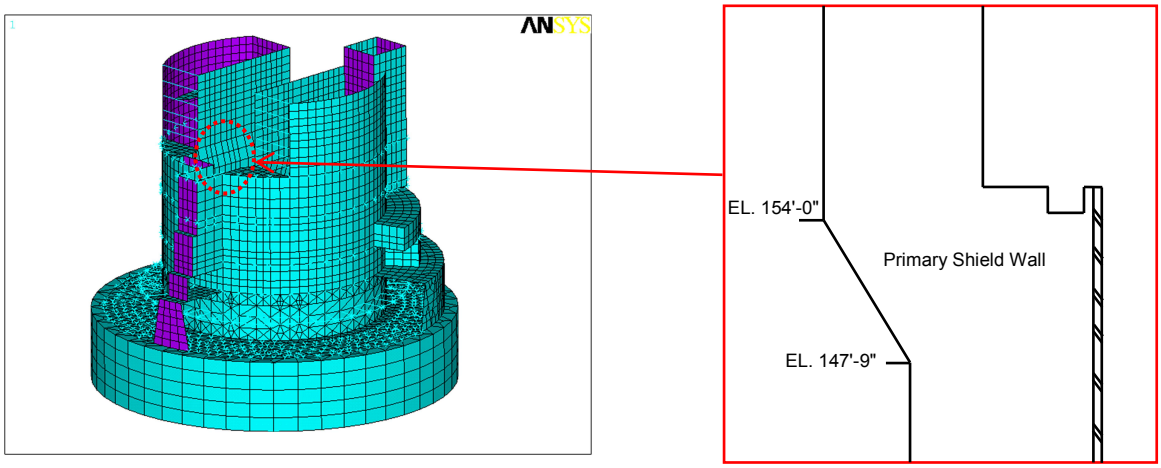

Figure 16. Tapered Section in Primary Shield Wall

d) The degrees of freedom compatibility condition between the beam elements of the reactor coolant system (RCS) and solid elements of the primary shield wall (PSW) and the secondary shield wall (SSW) was satisfied by using the rigid beam elements at the beam-to-wall support points covering the footprint of the RCS support brackets. The RCS supports are modeled as rigid beam elements and connected with other rigid beam elements in the solid elements which represent the PSW and the SSW.

Figure 17 shows the connection between the RCS supports (rigid beam) and the building model (solid elements). Technical report APR1400-E-S-NR-14002-P will be revised, as indicated in Attachment 3 to this response to incorporate the description of the beam-to-solid element connection.

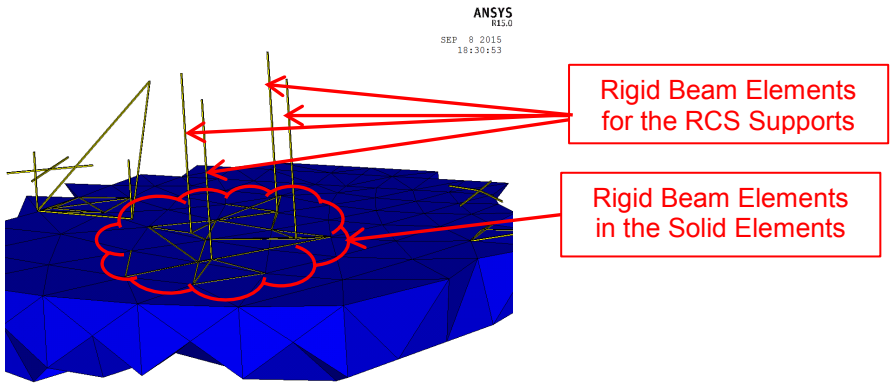

Figure 17. Connection between RCS Supports and Solid Elements

e) It is generally known that a dynamic Poisson's ratio value approaching 0.5 will cause numerical sensitivity problems in SSI analyses using the SASSI program. In the SSI analysis of the APR1400, the dynamic Poisson's ratio of the soil is limited to not greater than 0.48 in order to avoid numerical sensitivity problems. To demonstrate that the Poisson's ratio values used in the SSI analyses of S1 and S2 soil profile cases do not produce numerical instabilities in the SSI analysis results, a sensitivity study is performed using the ACS SASSI Nuclear Island (NI) model of APR1400 with S1 and S2 soil profiles.

In this sensitivity study, the S1 and S2 soil profiles which have the maximum Poisson's ratio values of 0.47 and 0.48 are modified to have maximum Poisson's ratio values of 0.45 and 0.42. In the sensitivity study, the shear wave (S-wave) and compression wave (P-wave) velocities of the soil layers in the ACS SASSI NI SSI model, which have the Poisson's ratio values greater than the assumed maximum Poisson's ratio values of 0.45 and 0.42, are modified to reduce the Poisson's ratio values of the soil layers. For the horizontal SSI analyses, the compression wave velocities are modified to meet the maximum Poisson's ratio values of 0.45 and 0.42. On the other hand, for the vertical SSI analyses, the shear wave velocities of soils in the SSI models are modified to meet the maximum Poisson's ratio values of 0.45 and 0.42. The modified shear and compression wave velocities of S1 and S2 soil profiles considered in the sensitivity study are presented in Tables 2 through 5.

Using the modified soil profiles of S1 and S2, SSI analyses of NI models of both cracked and uncracked concrete stiffness cases are re-performed. Then, the transfer function results at NI basemat bottom and plant grade elevations obtained from the original SSI analyses and the re-performed SSI analyses in the sensitivity study are compared to judge the existence of numerical instabilities in the original SSI results. The locations of the selected nodes at basemat bottom and plant grade elevations using in the comparisons are provided in Figures 18 and 19. The comparisons of transfer function results for S1 and S2 soil profile cases are presented in Figures 20 through 51.

As shown in the comparisons of transfer functions presented in these figures, the transfer functions obtained from the original SSI analyses are quite similar and comparable to the transfer functions obtained from the sensitivity study re-performed SSI analyses. In addition, no abrupt changes or spurious peaks, which tend to indicate existence of

numerical sensitivities in the SASSI solutions, appear in the computed transfer functions of the original SSI analyses that have the maximum dynamic Poisson's ratio values of 0.47 and 0.48 as well as in the re-computed transfer functions that have the maximum dynamic Poisson's ratio values limited to 0.42 and 0.45. These results demonstrate that there is no numerical instabilities in the original SSI analysis results of the S1 and S2 soil profile cases.

Table 2. Modified Shear and Compression Wave Velocities of the S1 Soil Profile Case for Maximum Poisson's Ratio Value of 0.42

Layer No.	Original S1 Profile		Modified S1 Profile for Horizontal Directional Analysis		Modified S1 Profile for Vertical Directional Analysis	
	S-Wave Velocities (ft/sec)	P-Wave Velocities (ft/sec)	S-Wave Velocities (ft/sec)	P-Wave Velocities (ft/sec)	S-Wave Velocities (ft/sec)	P-Wave Velocities (ft/sec)
1	1141	4800	1141	3072	1783	4800
2	1101	4800	1101	2965	1783	4800
3	1139	4800	1139	3067	1783	4800
4	1141	4800	1141	3072	1783	4800
5	1174	4800	1174	3161	1783	4800
6	1229	4800	1229	3309	1783	4800
7	1234	4800	1234	3323	1783	4800
8	1246	4800	1246	3355	1783	4800
9	1257	4800	1257	3385	1783	4800
10	1271	4800	1271	3422	1783	4800
11	1285	4800	1285	3460	1783	4800
12	1299	4800	1299	3498	1783	4800
13	1314	4800	1314	3538	1783	4800
14	1328	4800	1328	3576	1783	4800
15	1342	4800	1342	3613	1783	4800
16	1357	4800	1357	3654	1783	4800
17	1373	4800	1373	3697	1783	4800
18	1389	4800	1389	3740	1783	4800
19	1406	4800	1406	3786	1783	4800
20	1489	4800	1489	4009	1783	4800
21	1506	4800	1506	4055	1783	4800
22	1523	4800	1523	4101	1783	4800
23	1540	4800	1540	4147	1783	4800
24	1556	4800	1556	4190	1783	4800
25	1573	4800	1573	4235	1783	4800
26	1590	4800	1590	4281	1783	4800
27	1608	4800	1608	4330	1783	4800
28	1625	4800	1625	4375	1783	4800
29	1642	4800	1642	4421	1783	4800
30	1659	4800	1659	4467	1783	4800
31	1676	4800	1676	4513	1783	4800
32	1692	4800	1692	4556	1783	4800
33	1709	4800	1709	4602	1783	4800
34	1725	4800	1725	4645	1783	4800
35	1742	4845	1742	4690	1799	4845

Table 3. Modified Shear and Compression Wave Velocities of the S1 Soil Profile Case for Maximum Poisson's Ratio Value of 0.45

Layer No.	Original S1 Profile		Modified S1 Profile for Horizontal Directional Analysis		Modified S1 Profile for Vertical Directional Analysis	
	S-Wave Velocities (ft/sec)	P-Wave Velocities (ft/sec)	S-Wave Velocities (ft/sec)	P-Wave Velocities (ft/sec)	S-Wave Velocities (ft/sec)	P-Wave Velocities (ft/sec)
1	1141	4800	1141	3784	1447	4800
2	1101	4800	1101	3652	1447	4800
3	1139	4800	1139	3778	1447	4800
4	1141	4800	1141	3784	1447	4800
5	1174	4800	1174	3894	1447	4800
6	1229	4800	1229	4076	1447	4800
7	1234	4800	1234	4093	1447	4800
8	1246	4800	1246	4133	1447	4800
9	1257	4800	1257	4169	1447	4800
10	1271	4800	1271	4215	1447	4800
11	1285	4800	1285	4262	1447	4800
12	1299	4800	1299	4308	1447	4800
13	1314	4800	1314	4358	1447	4800
14	1328	4800	1328	4404	1447	4800
15	1342	4800	1342	4451	1447	4800
16	1357	4800	1357	4501	1447	4800
17	1373	4800	1373	4554	1447	4800
18	1389	4800	1389	4607	1447	4800
19	1406	4800	1406	4663	1447	4800

Table 4. Modified Shear and Compression Wave Velocities of the S2 Soil Profile Case for Maximum Poisson's Ratio Value of 0.42

Layer No.	Original S2 Profile		Modified S2 Profile for Horizontal Directional Analysis		Modified S2 Profile for Vertical Directional Analysis	
	S-Wave Velocities (ft/sec)	P-Wave Velocities (ft/sec)	S-Wave Velocities (ft/sec)	P-Wave Velocities (ft/sec)	S-Wave Velocities (ft/sec)	P-Wave Velocities (ft/sec)
1	975	4800	975	2625	1783	4800
2	921	4800	921	2480	1783	4800
3	951	4800	951	2561	1783	4800
4	947	4800	947	2550	1783	4800
5	975	4800	975	2625	1783	4800
6	1029	4800	1029	2771	1783	4800
7	1034	4800	1034	2784	1783	4800
8	1044	4800	1044	2811	1783	4800
9	1054	4800	1054	2838	1783	4800
10	1065	4800	1065	2868	1783	4800
11	1075	4800	1075	2895	1783	4800
12	1086	4800	1086	2924	1783	4800
13	1098	4800	1098	2956	1783	4800
14	1110	4800	1110	2989	1783	4800
15	1123	4800	1123	3024	1783	4800

Table 5. Modified Shear and Compression Wave Velocities of the S2 Soil Profile Case for Maximum Poisson's Ratio Value of 0.45

Layer No.	Original S2 Profile		Modified S2 Profile for Horizontal Directional Analysis		Modified S2 Profile for Vertical Directional Analysis	
	S-Wave Velocities (ft/sec)	P-Wave Velocities (ft/sec)	S-Wave Velocities (ft/sec)	P-Wave Velocities (ft/sec)	S-Wave Velocities (ft/sec)	P-Wave Velocities (ft/sec)
1	975	4800	975	3234	1447	4800
2	921	4800	921	3055	1447	4800
3	951	4800	951	3154	1447	4800
4	947	4800	947	3141	1447	4800
5	975	4800	975	3234	1447	4800
6	1029	4800	1029	3413	1447	4800
7	1034	4800	1034	3429	1447	4800
8	1044	4800	1044	3463	1447	4800
9	1054	4800	1054	3496	1447	4800
10	1065	4800	1065	3532	1447	4800
11	1075	4800	1075	3565	1447	4800
12	1086	4800	1086	3602	1447	4800
13	1098	4800	1098	3642	1447	4800
14	1110	4800	1110	3681	1447	4800
15	1123	4800	1123	3725	1447	4800

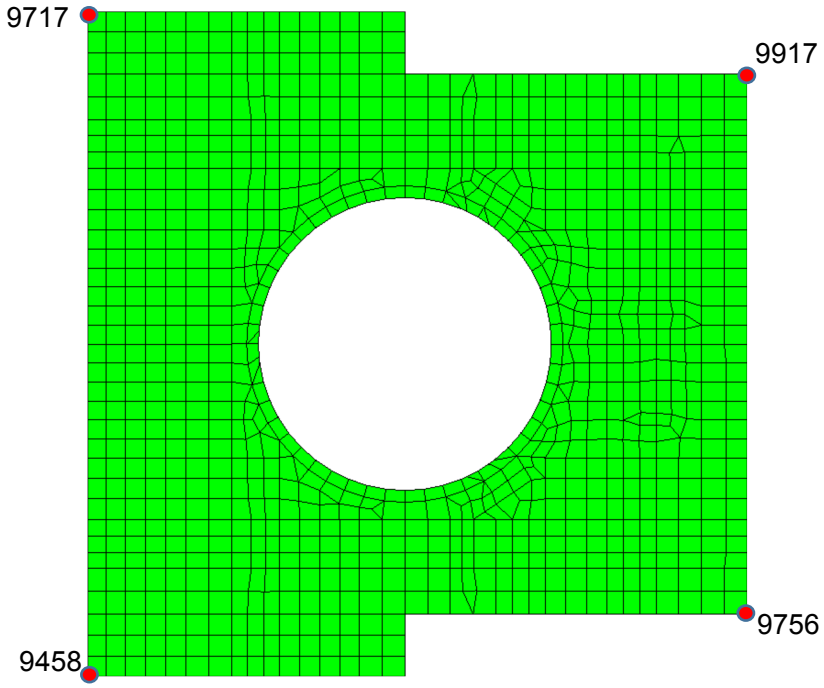

Figure 18. Selected Nodes at Basemat Bottom Elevation for Comparisons of Transfer Functions

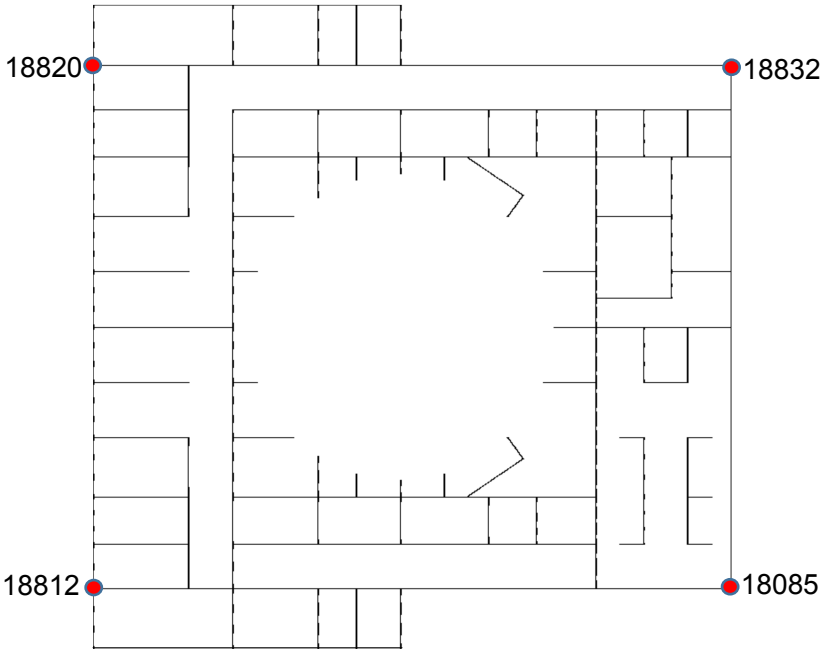

Figure 19. Selected Nodes at Plant Grade Elevation for Comparisons of Transfer Functions

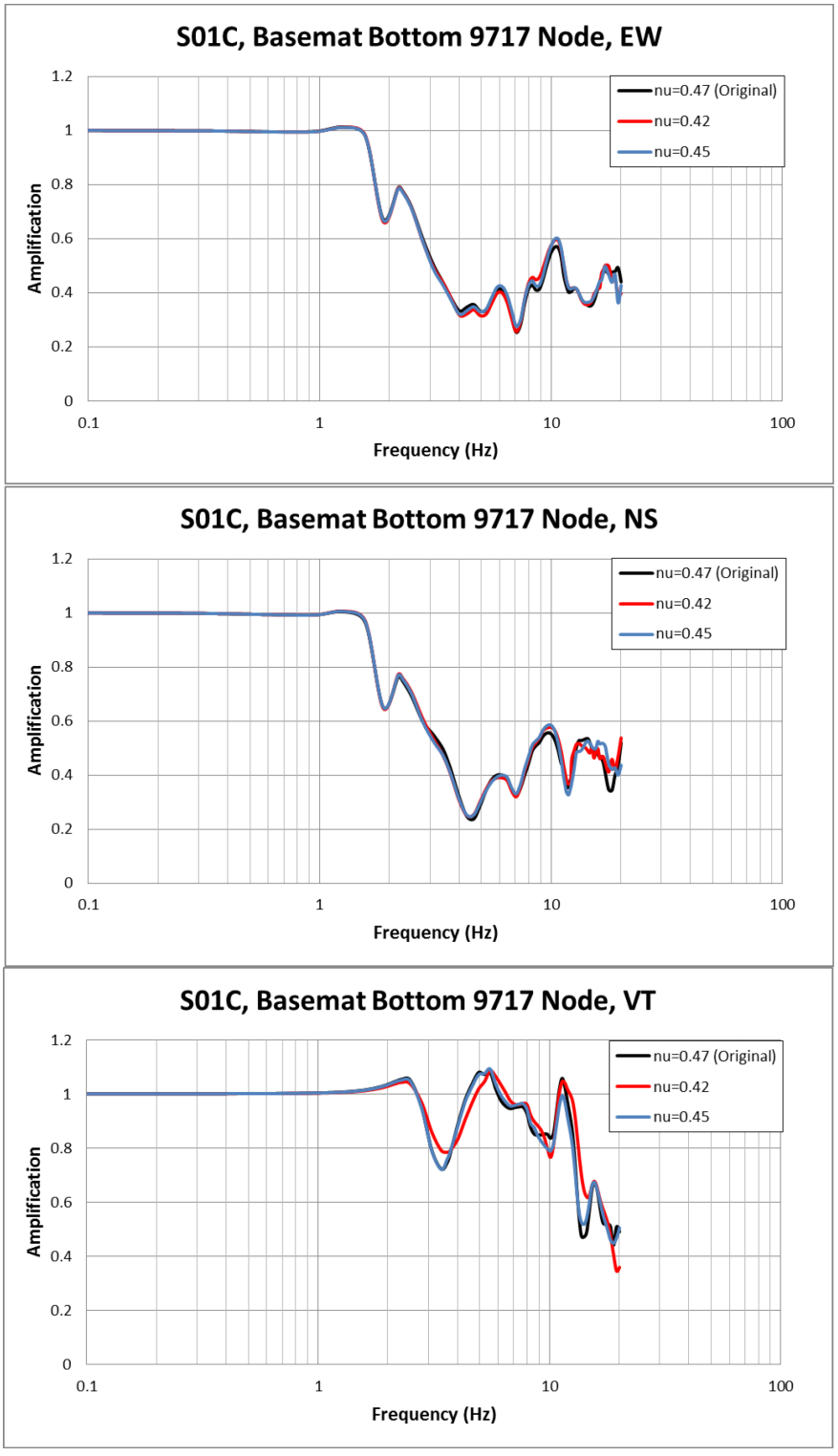

Figure 20. Comparison of Transfer Functions of 9717 Node at Basemat Bottom Elevation (S1 Soil Profile, Cracked Concrete Stiffness Case)

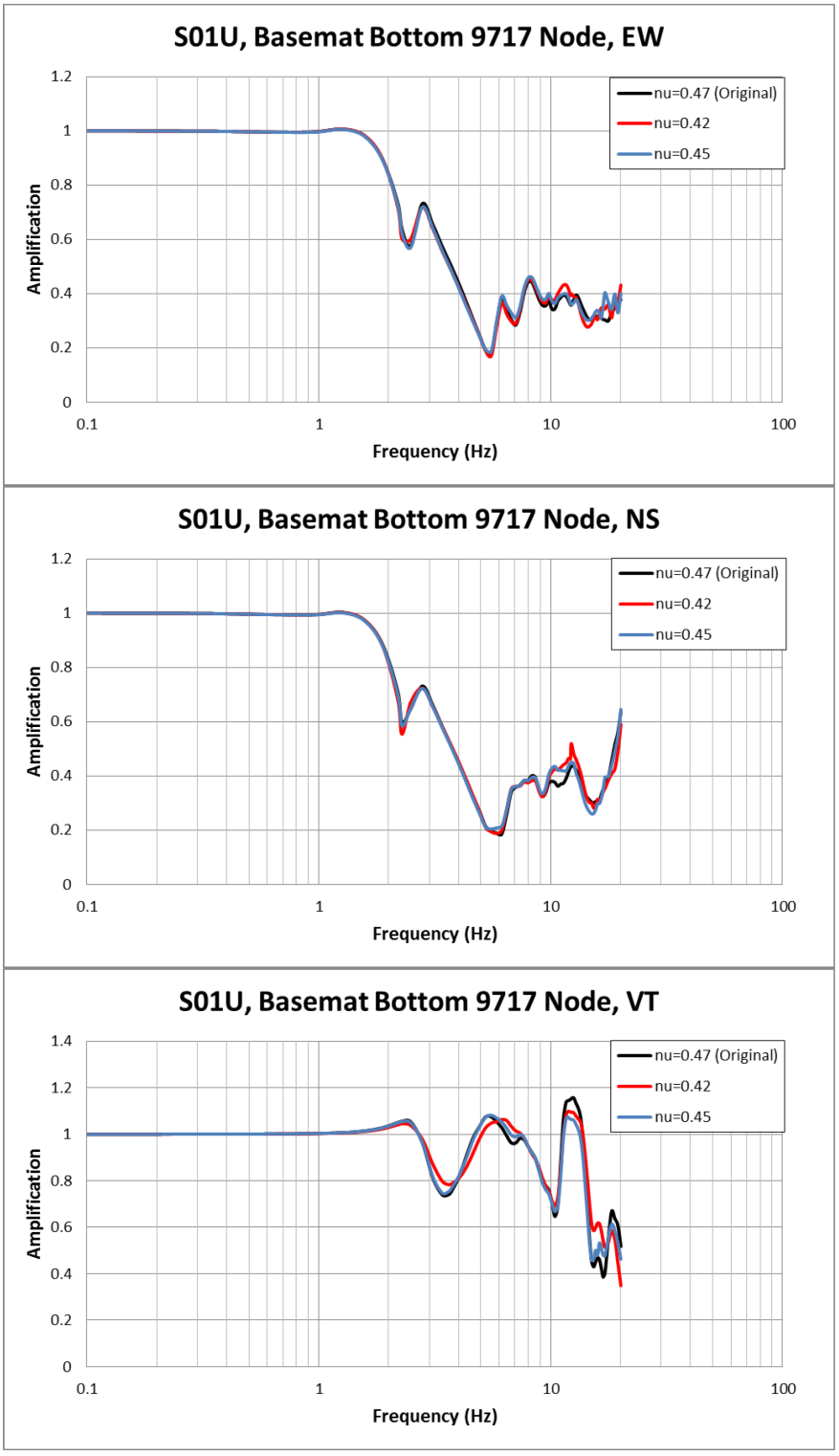

Figure 21. Comparison of Transfer Functions of 9717 Node at Basemat Bottom Elevation (S1 Soil Profile, Uncracked Concrete Stiffness Case)

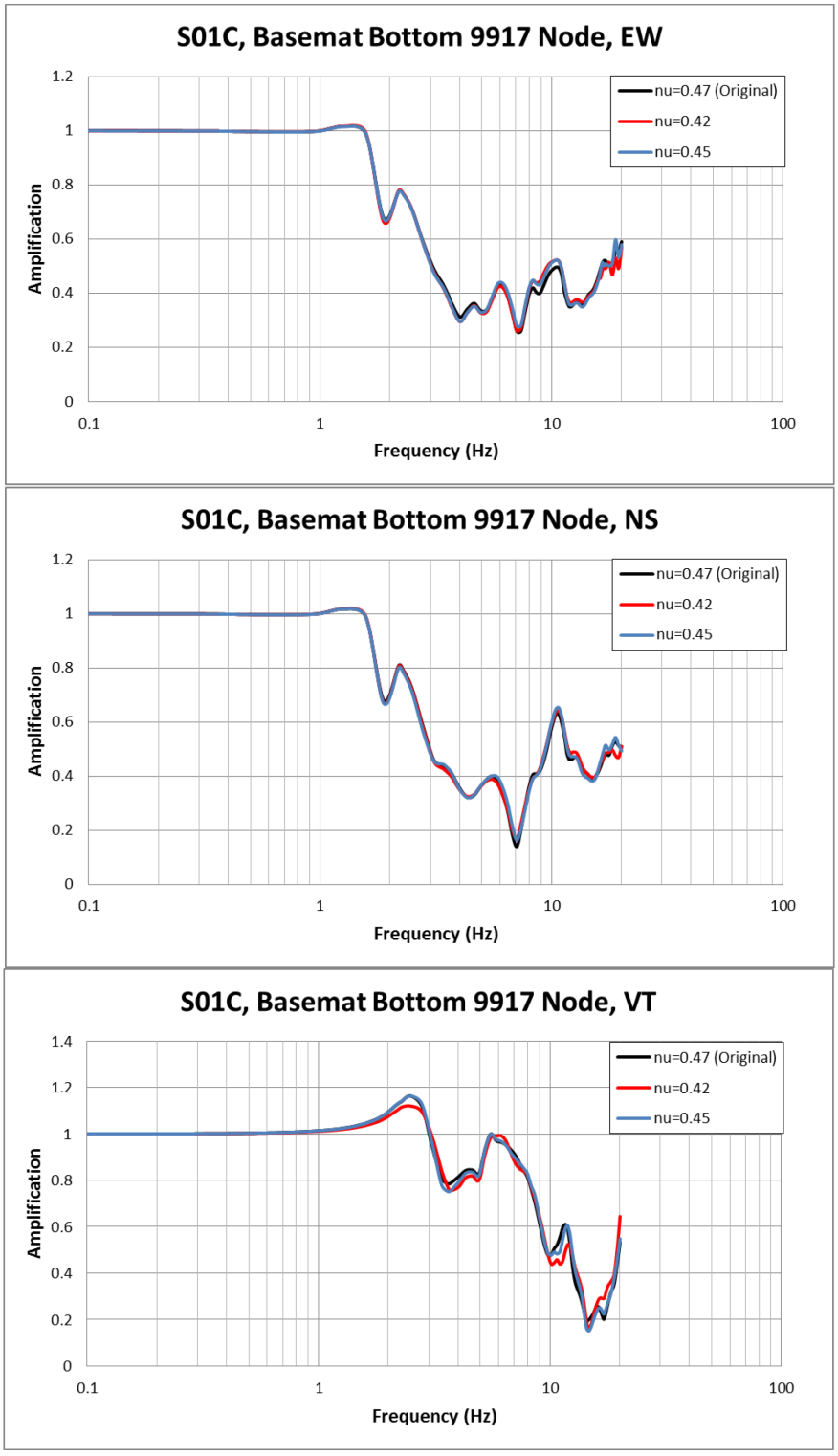

Figure 22. Comparison of Transfer Functions of 9917 Node at Basemat Bottom Elevation (S1 Soil Profile, Cracked Concrete Stiffness Case)

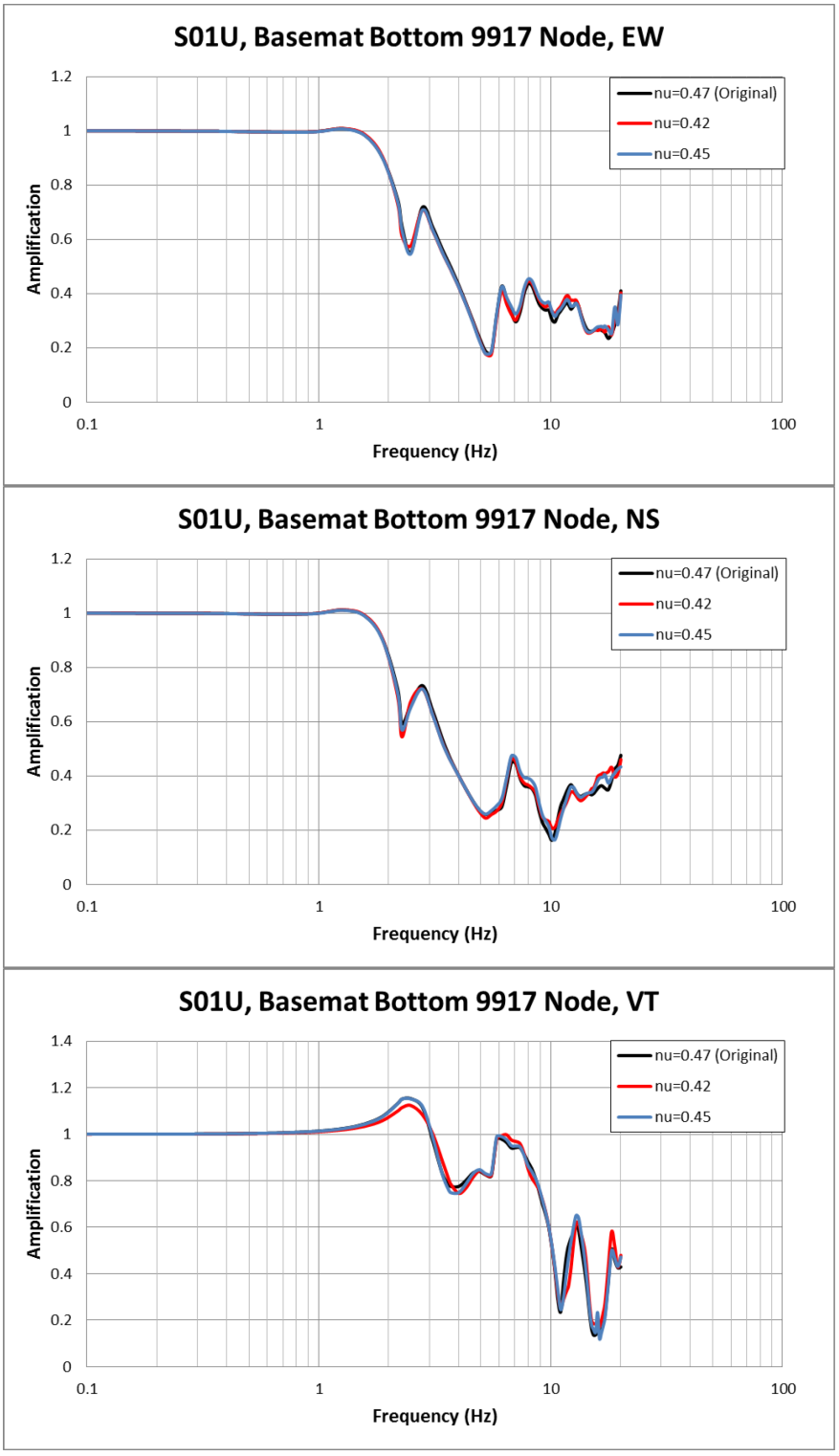

Figure 23. Comparison of Transfer Functions of 9917 Node at Basemat Bottom Elevation (S1 Soil Profile, Uncracked Concrete Stiffness Case)

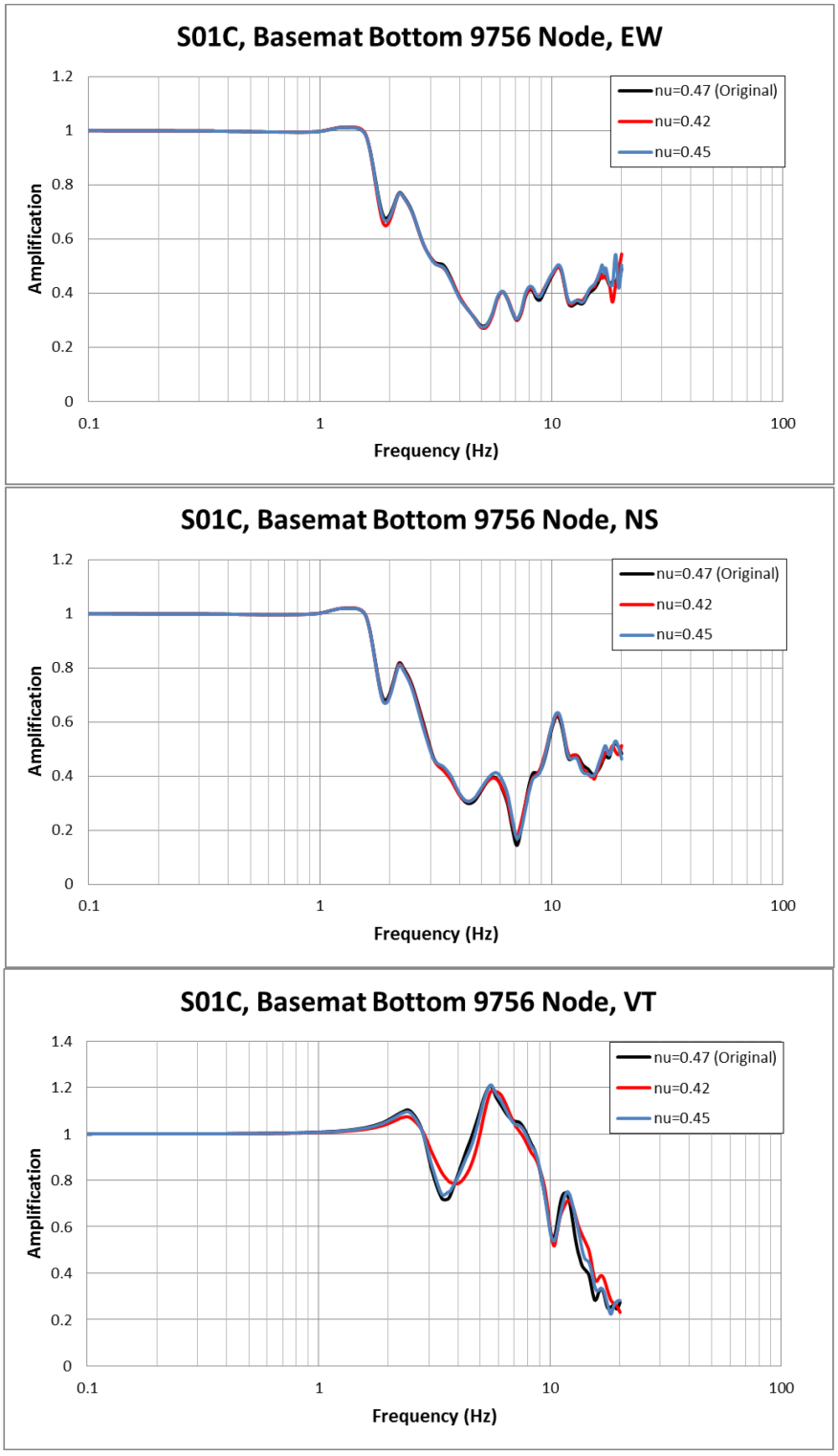

Figure 24. Comparison of Transfer Functions of 9756 Node at Basemat Bottom Elevation (S1 Soil Profile, Cracked Concrete Stiffness Case)

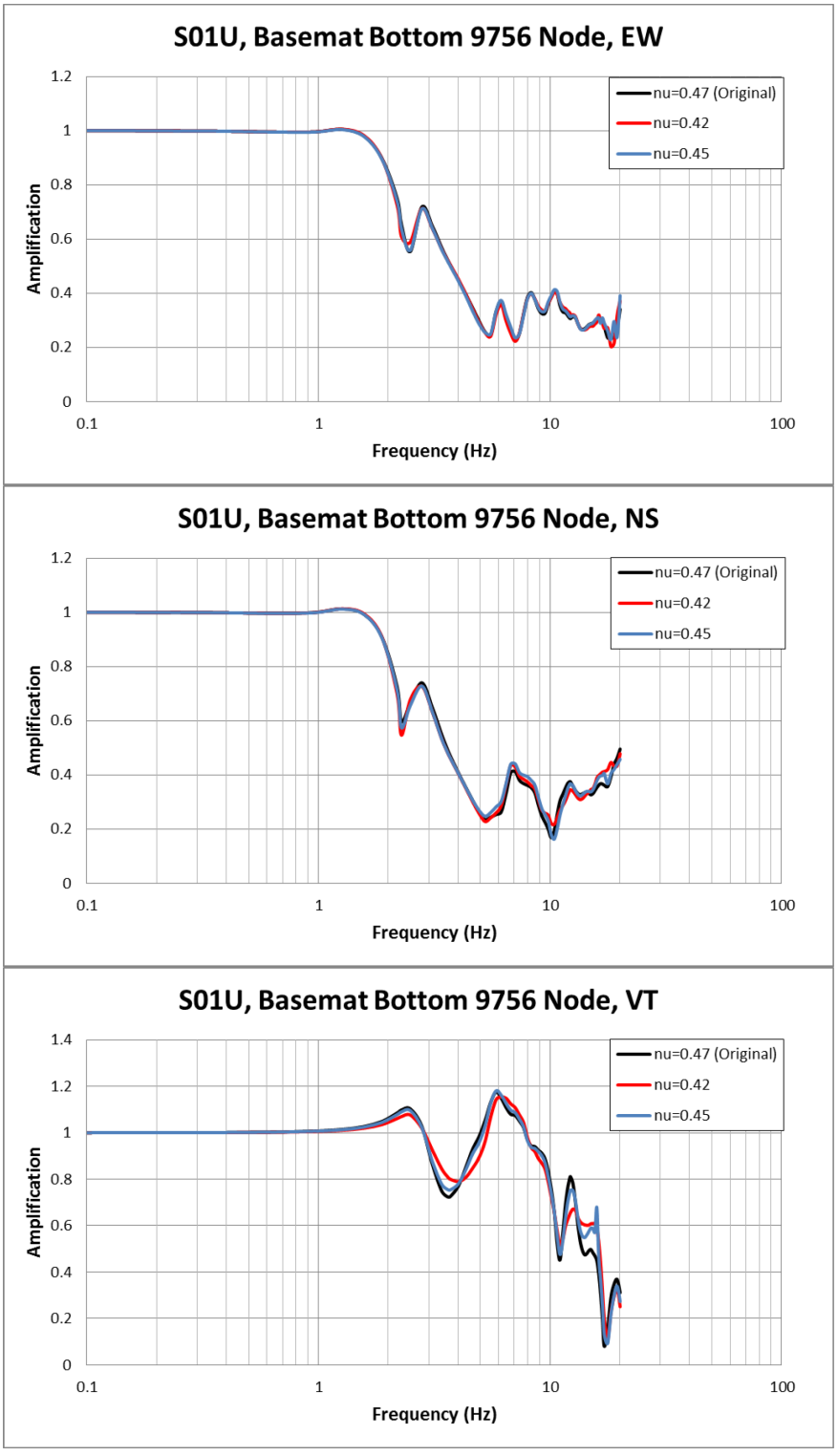

Figure 25. Comparison of Transfer Functions of 9756 Node at Basemat Bottom Elevation (S1 Soil Profile, Uncracked Concrete Stiffness Case)

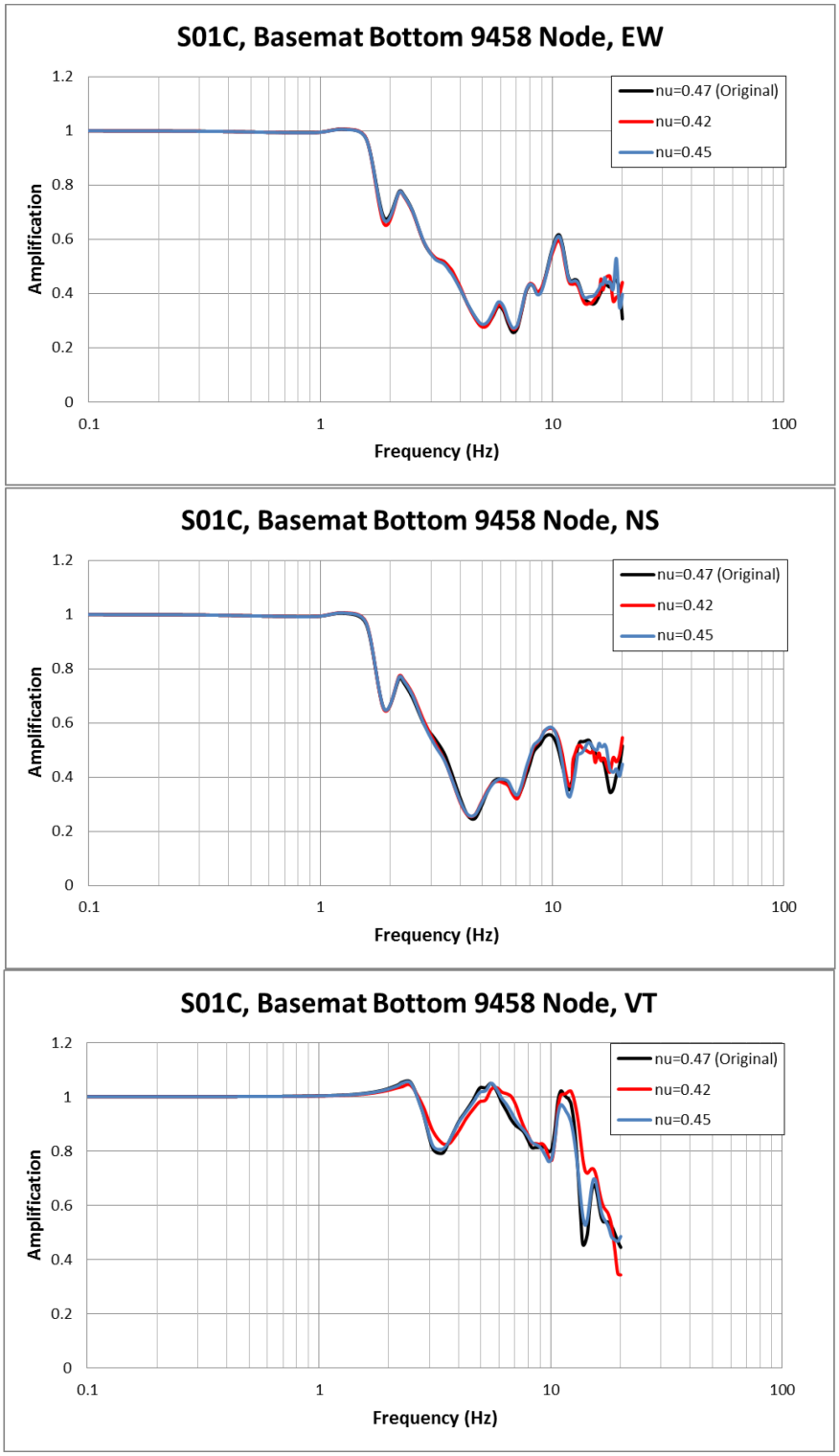

Figure 26. Comparison of Transfer Functions of 9458 Node at Basemat Bottom Elevation (S1 Soil Profile, Cracked Concrete Stiffness Case)

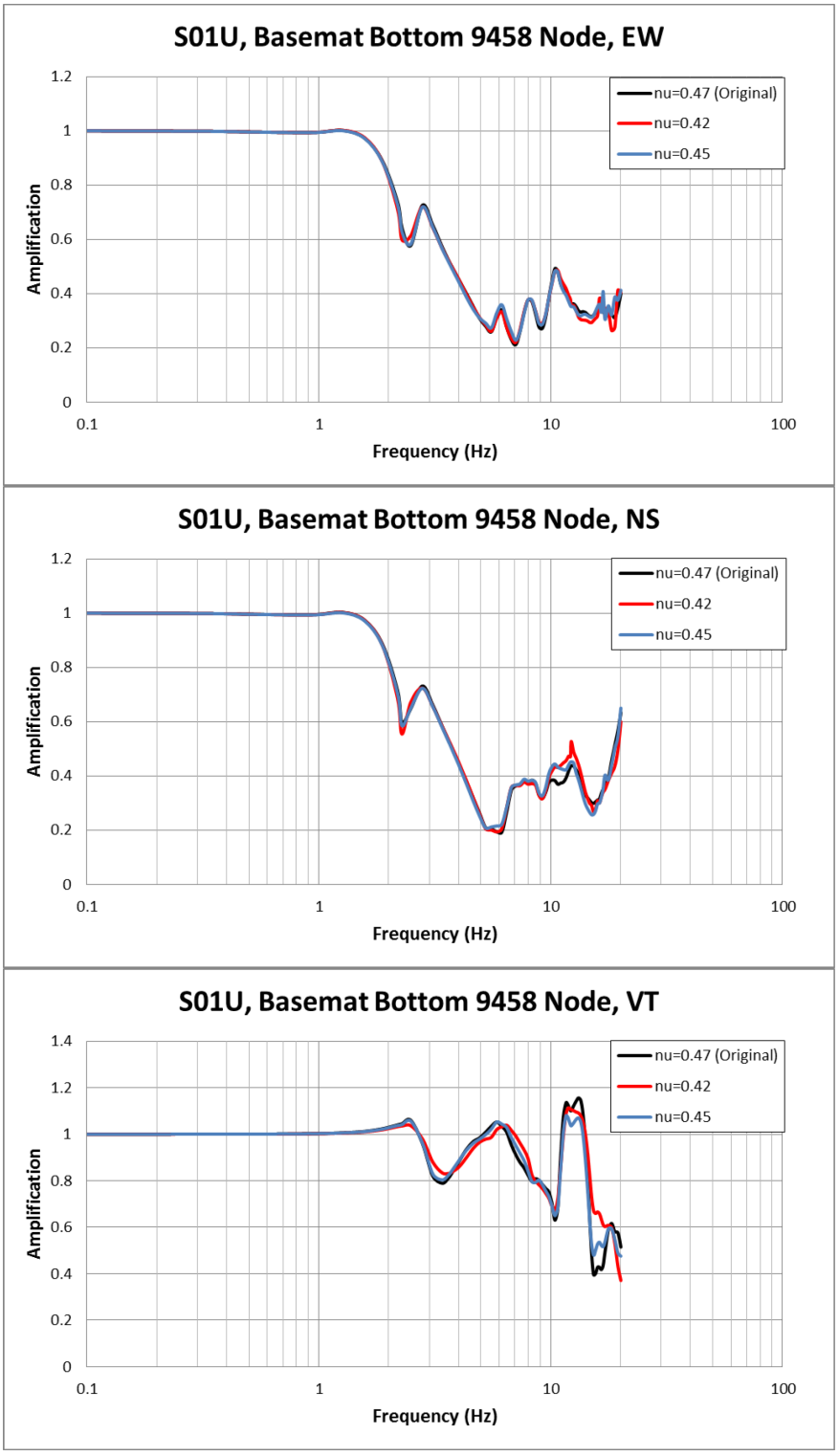

Figure 27. Comparison of Transfer Functions of 9458 Node at Basemat Bottom Elevation (S1 Soil Profile, Uncracked Concrete Stiffness Case)

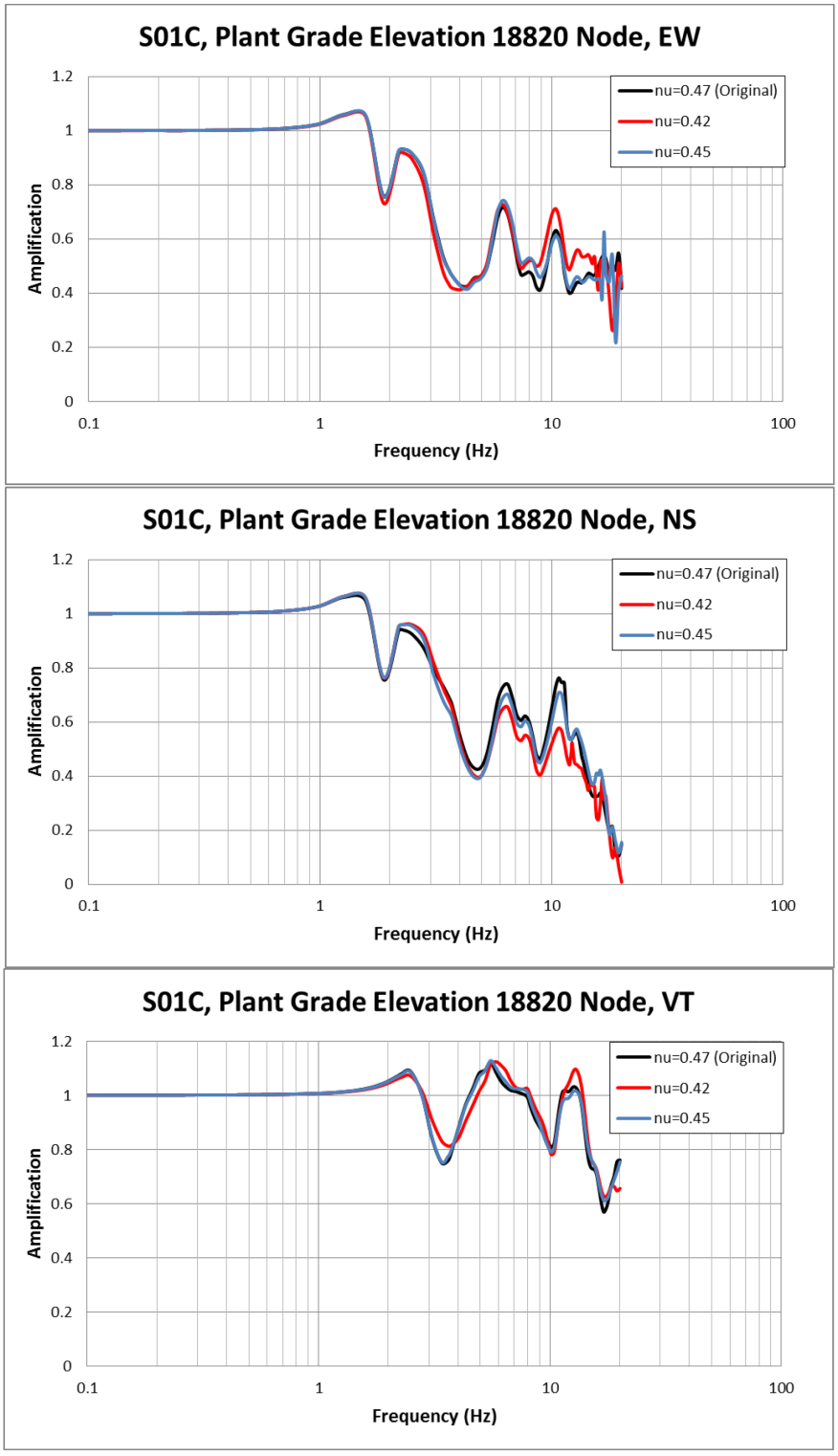

Figure 28. Comparison of Transfer Functions of 18820 Node at Plant Grade Elevation (S1 Soil Profile, Cracked Concrete Stiffness Case)

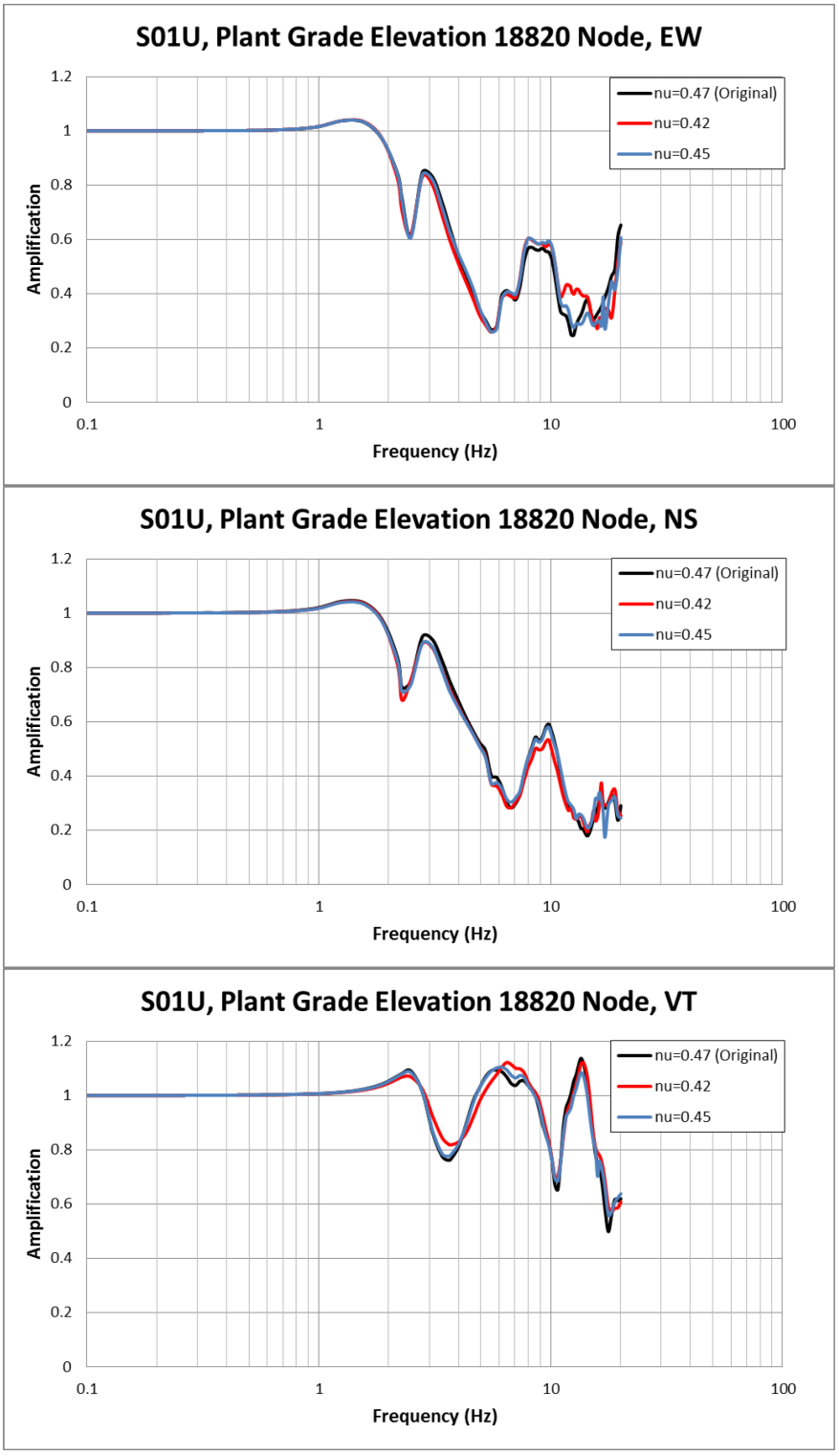

Figure 29. Comparison of Transfer Functions of 18820 Node at Plant Grade Elevation (S1 Soil Profile, Uncracked Concrete Stiffness Case)

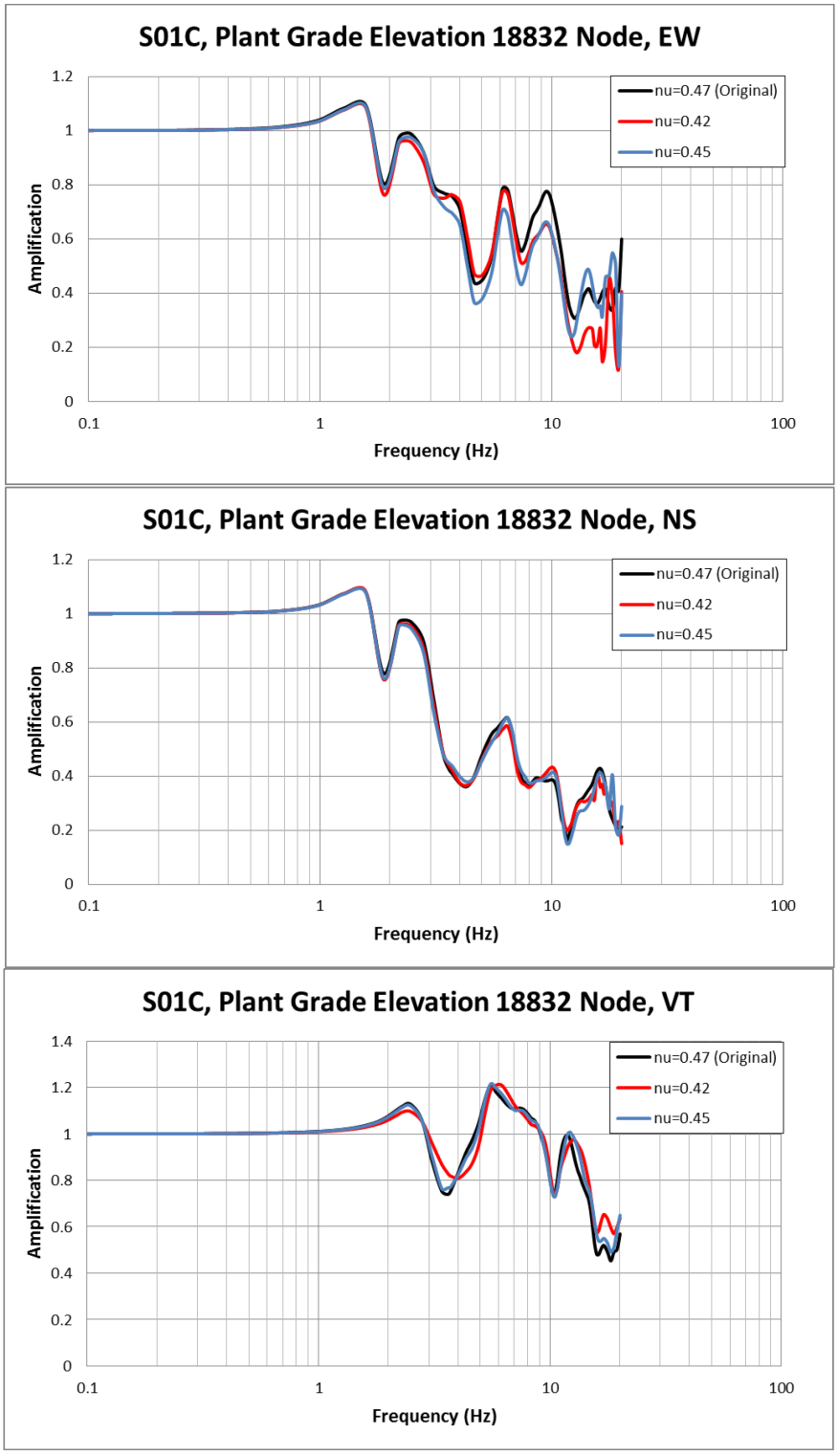

Figure 30. Comparison of Transfer Functions of 18832 Node at Plant Grade Elevation (S1 Soil Profile, Cracked Concrete Stiffness Case)

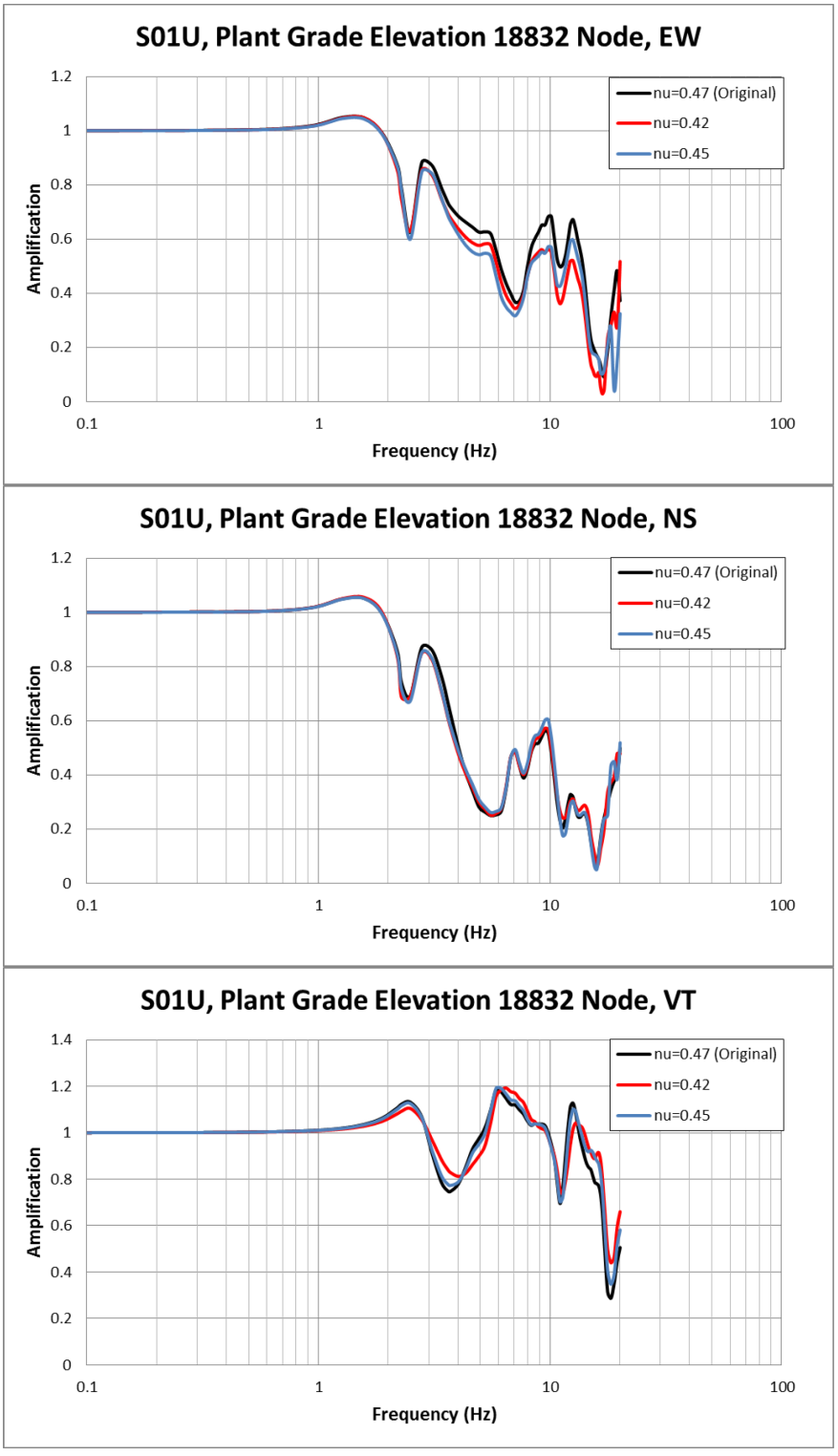

Figure 31. Comparison of Transfer Functions of 18832 Node at Plant Grade Elevation (S1 Soil Profile, Uncracked Concrete Stiffness Case)

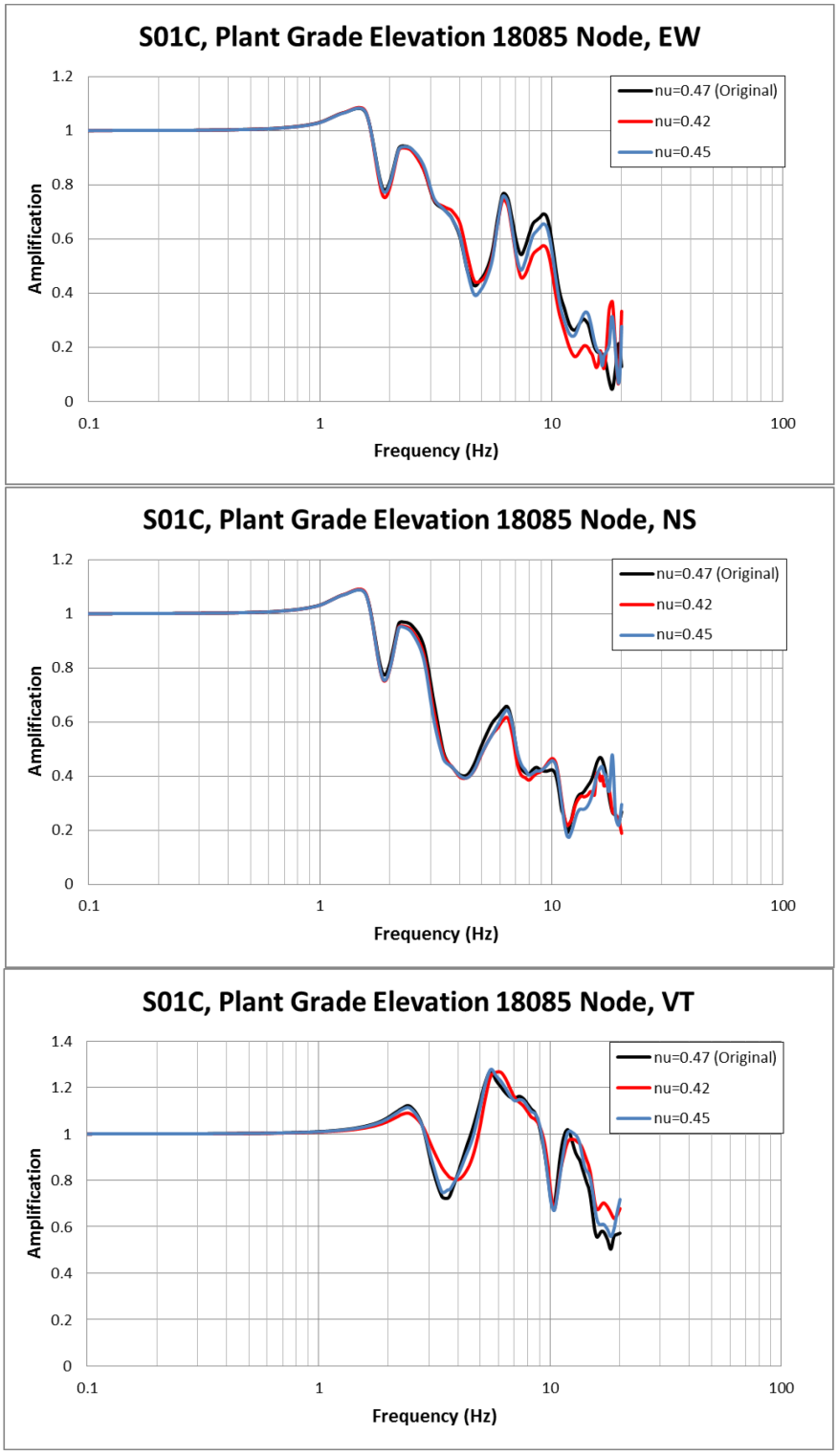

Figure 32. Comparison of Transfer Functions of 18085 Node at Plant Grade Elevation (S1 Soil Profile, Cracked Concrete Stiffness Case)

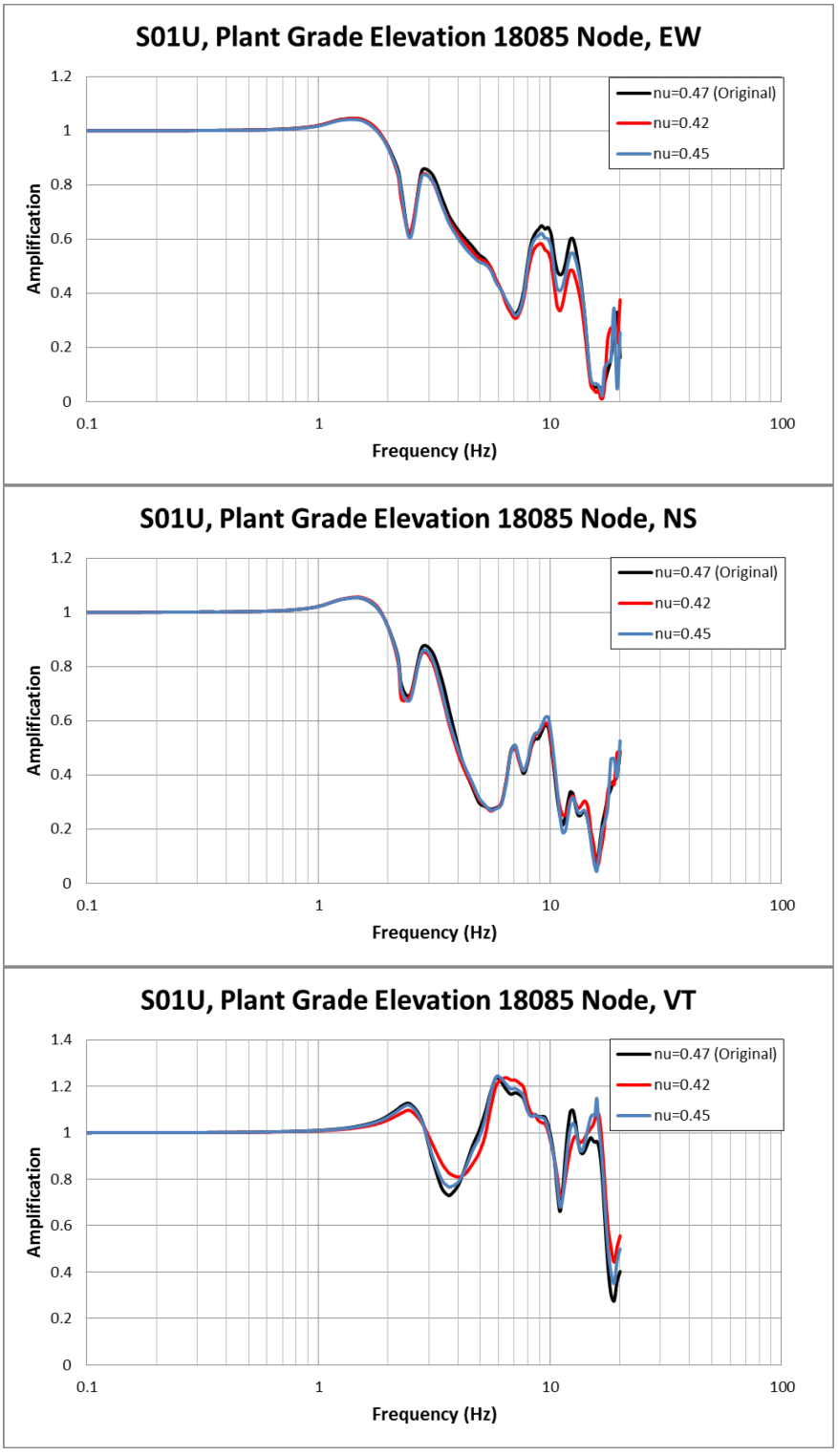

Figure 33. Comparison of Transfer Functions of 18085 Node at Plant Grade Elevation (S1 Soil Profile, Uncracked Concrete Stiffness Case)

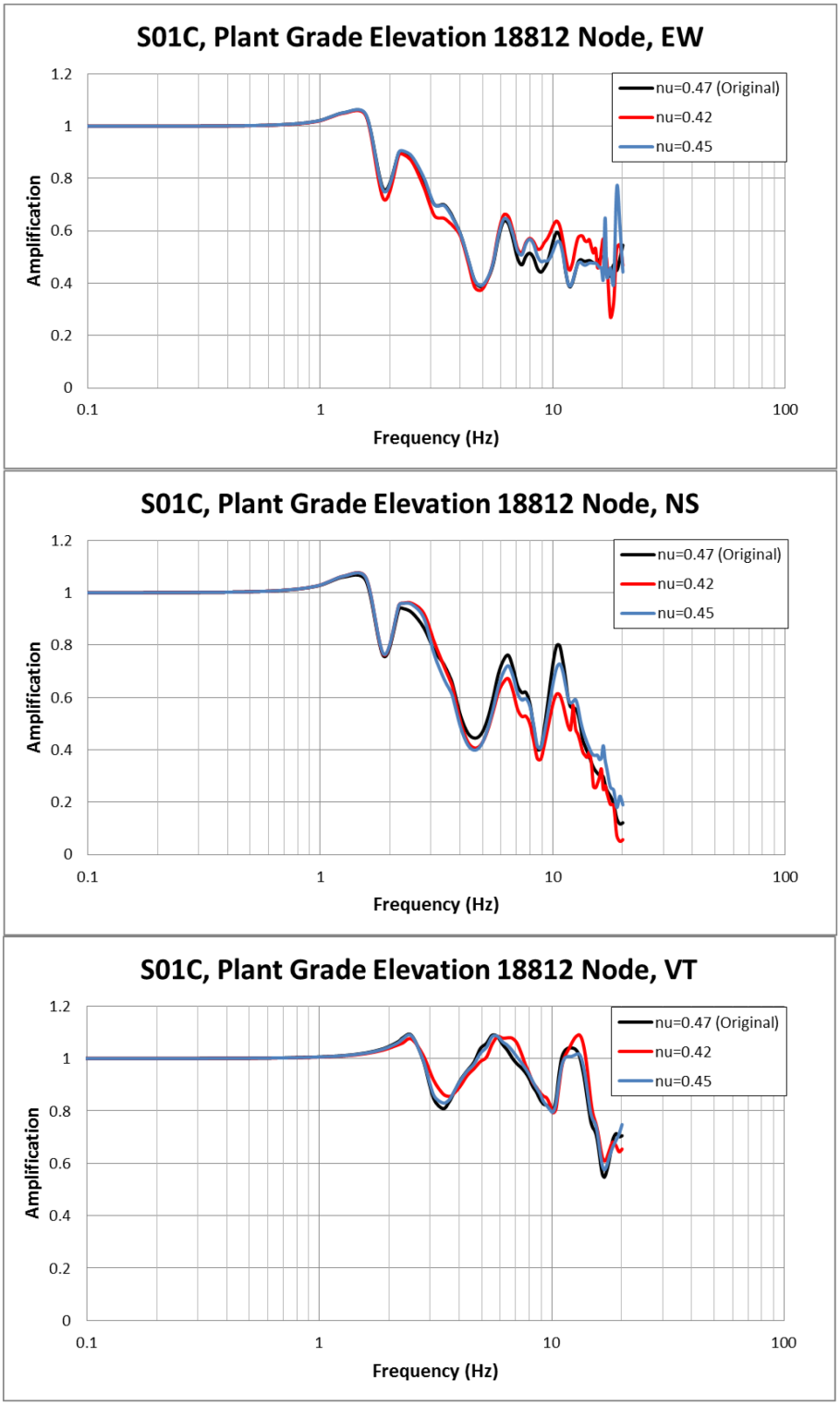

Figure 34. Comparison of Transfer Functions of 18812 Node at Plant Grade Elevation (S1 Soil Profile, Cracked Concrete Stiffness Case)

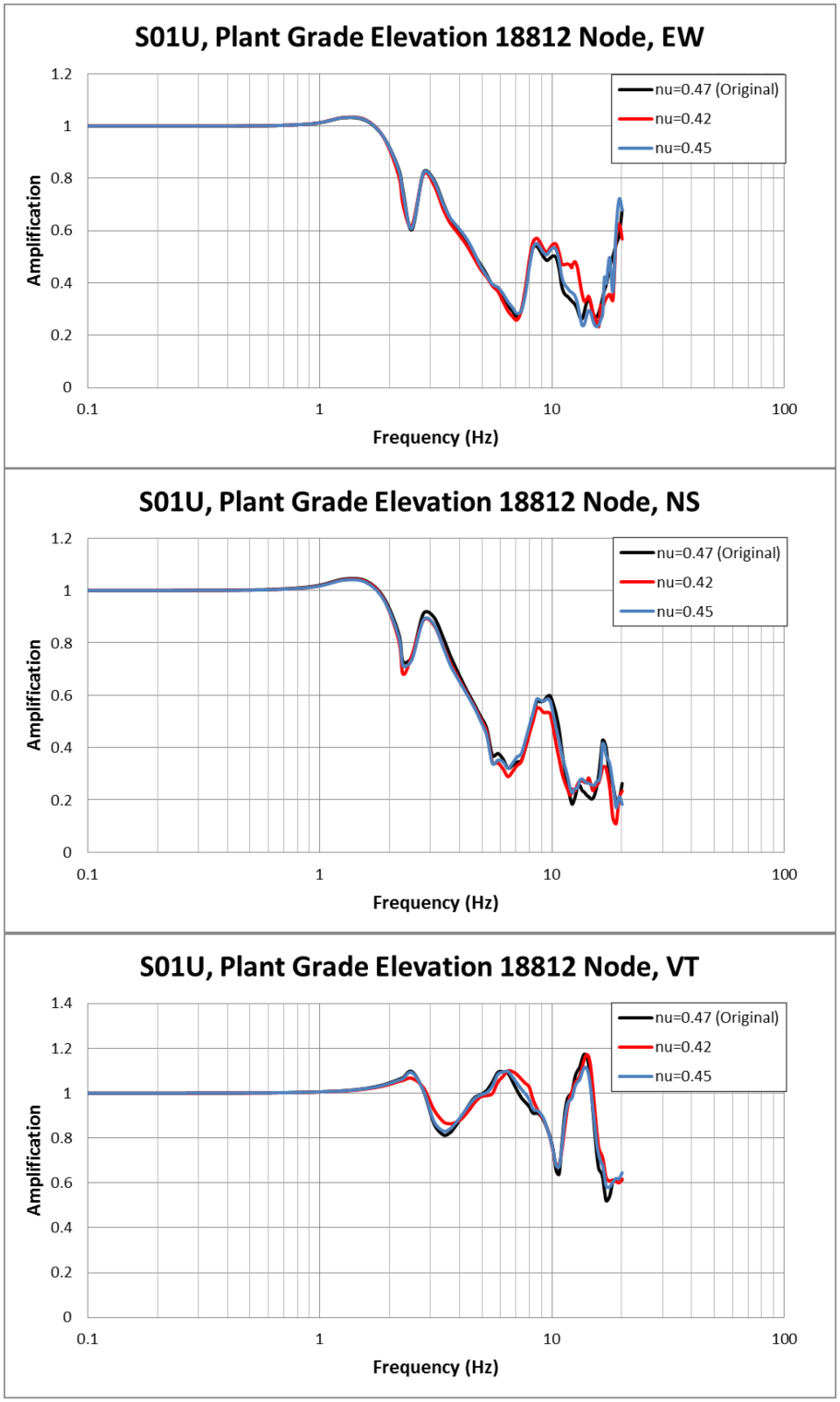

Figure 35. Comparison of Transfer Functions of 18812 Node at Plant Grade Elevation (S1 Soil Profile, Uncracked Concrete Stiffness Case)

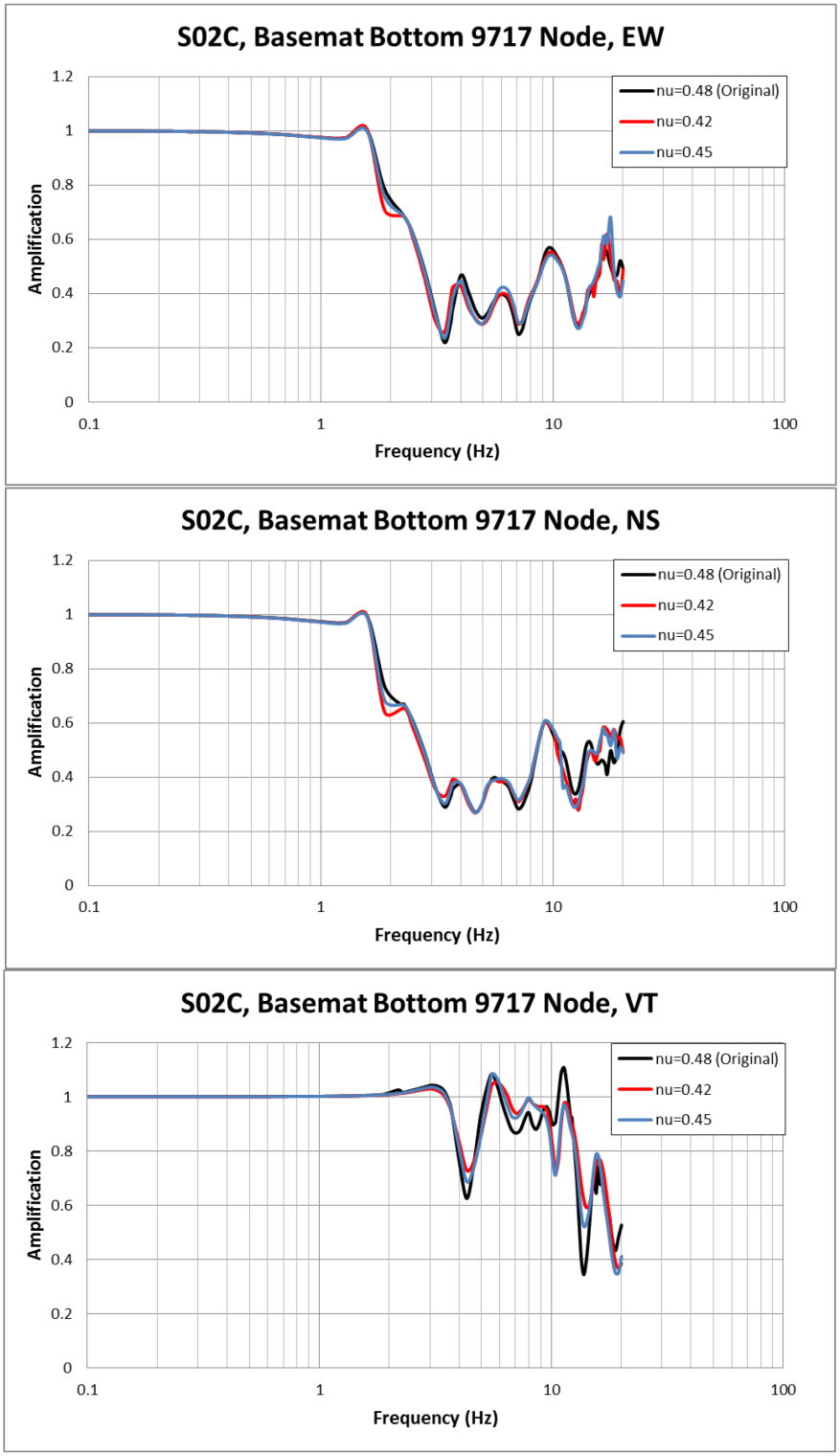

Figure 36. Comparison of Transfer Functions of 9717 Node at Basemat Bottom Elevation (S2 Soil Profile, Cracked Concrete Stiffness Case)

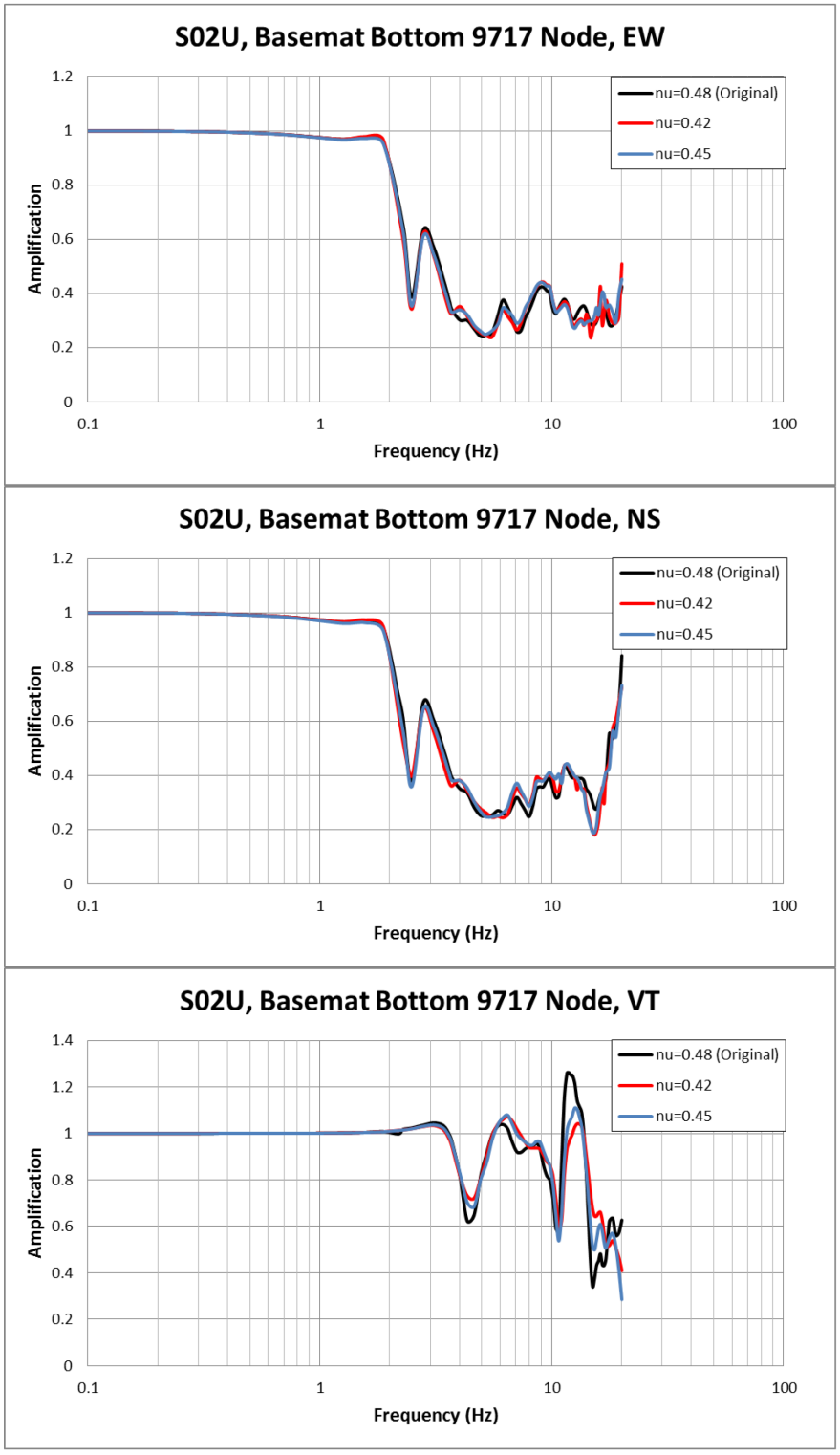

Figure 37. Comparison of Transfer Functions of 9717 Node at Basemat Bottom Elevation (S2 Soil Profile, Uncracked Concrete Stiffness Case)

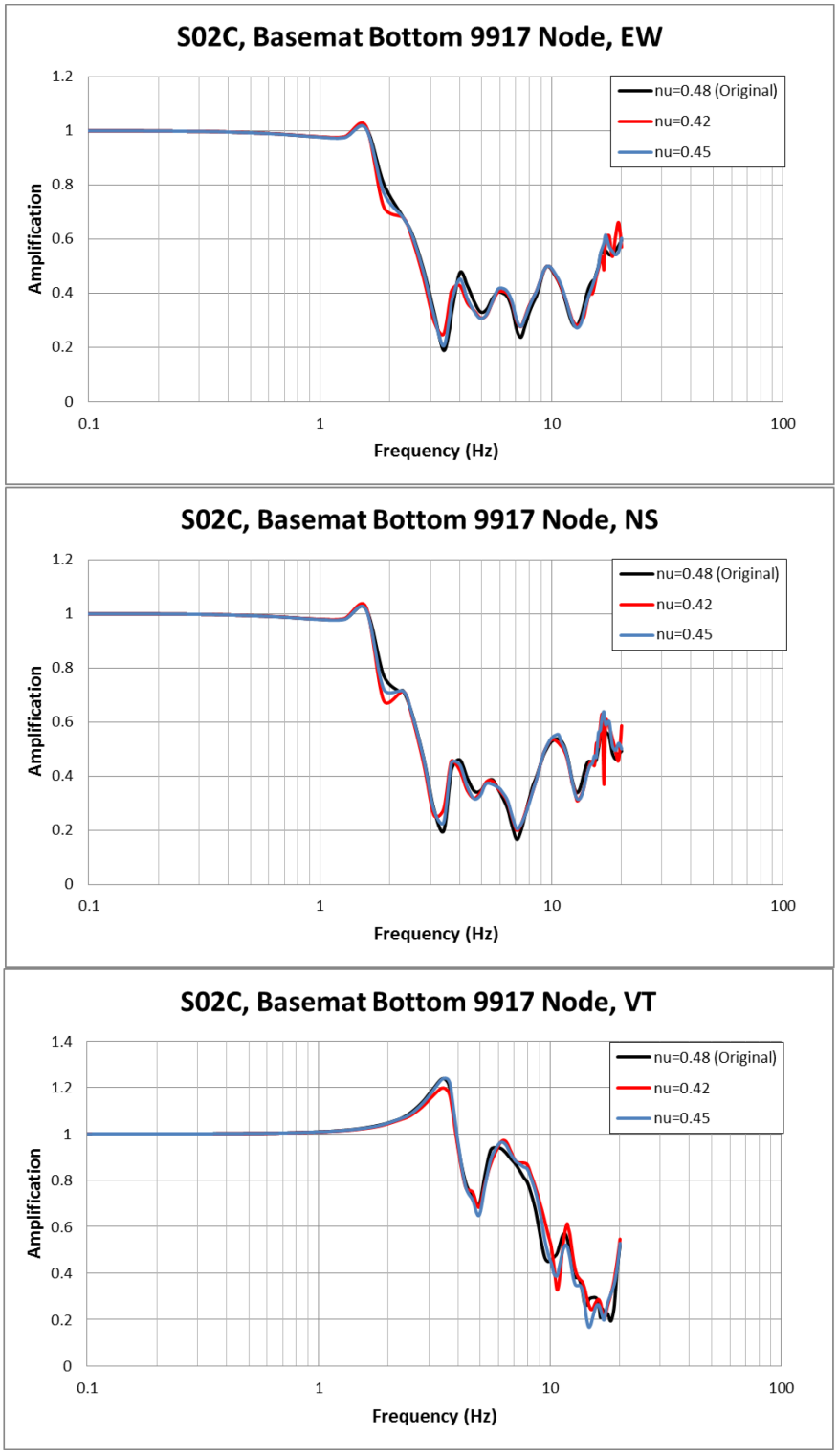

Figure 38. Comparison of Transfer Functions of 9917 Node at Basemat Bottom Elevation (S2 Soil Profile, Cracked Concrete Stiffness Case)

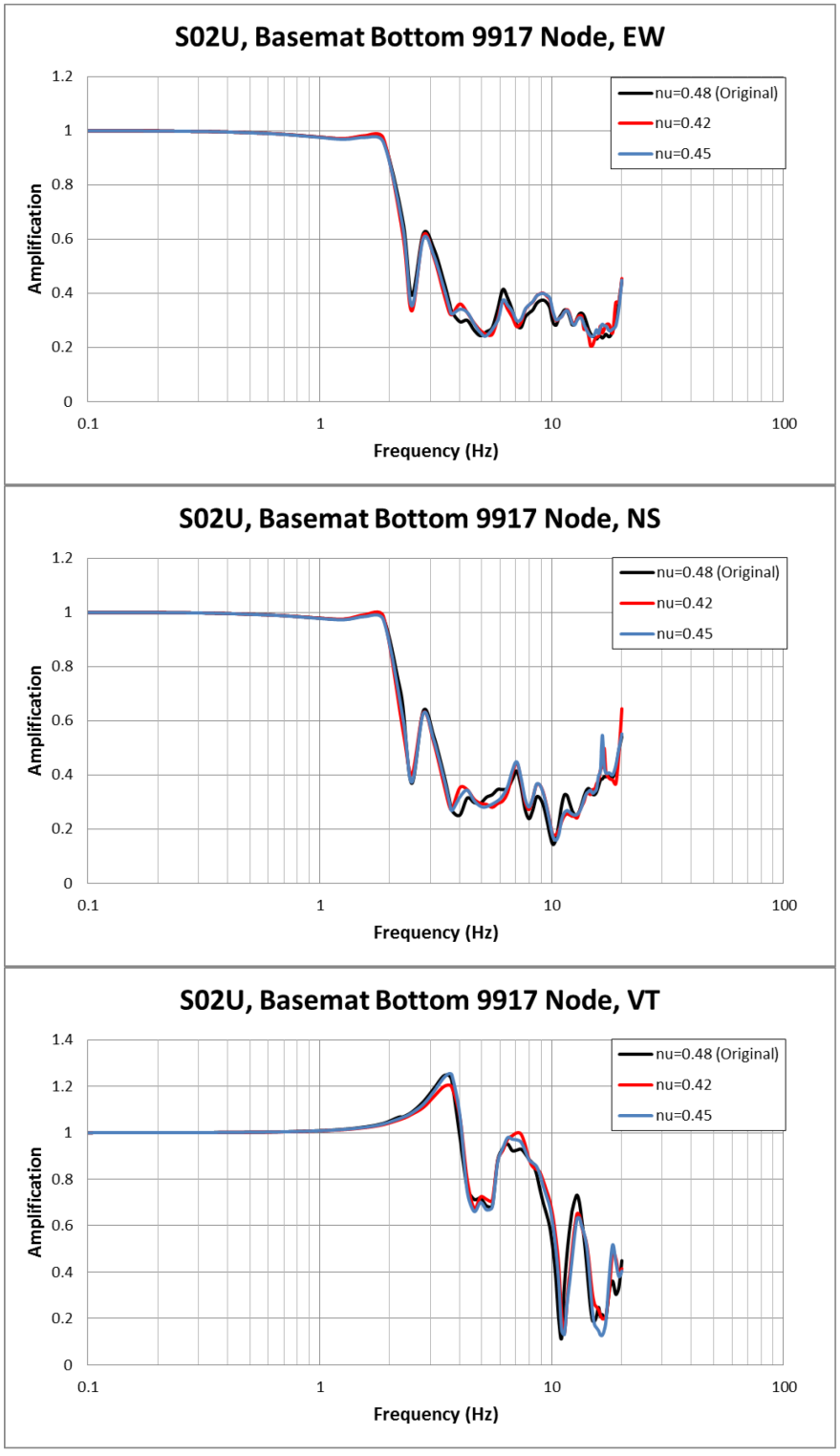

Figure 39. Comparison of Transfer Functions of 9917 Node at Basemat Bottom Elevation (S2 Soil Profile, Uncracked Concrete Stiffness Case)

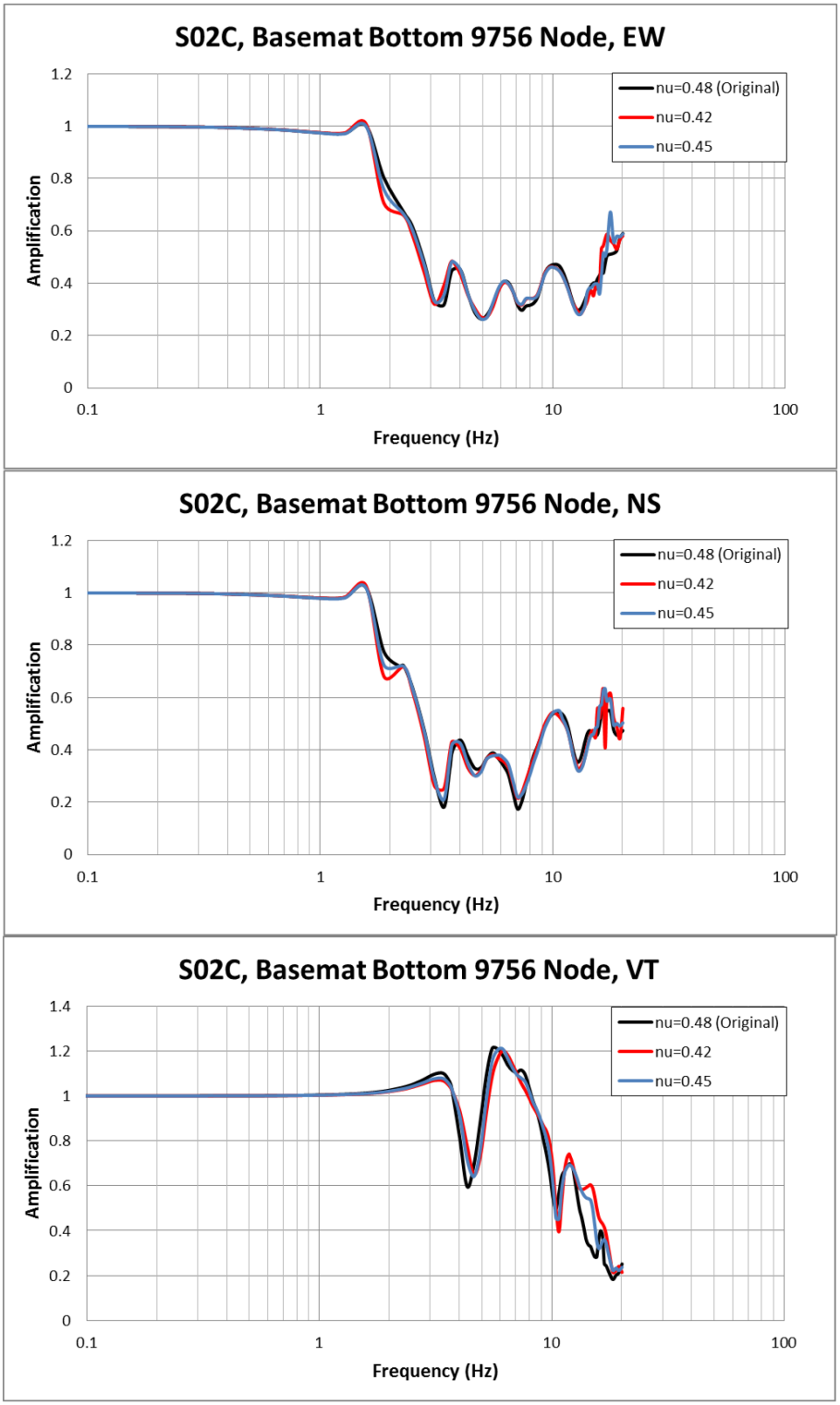

Figure 40. Comparison of Transfer Functions of 9756 Node at Basemat Bottom Elevation (S2 Soil Profile, Cracked Concrete Stiffness Case)

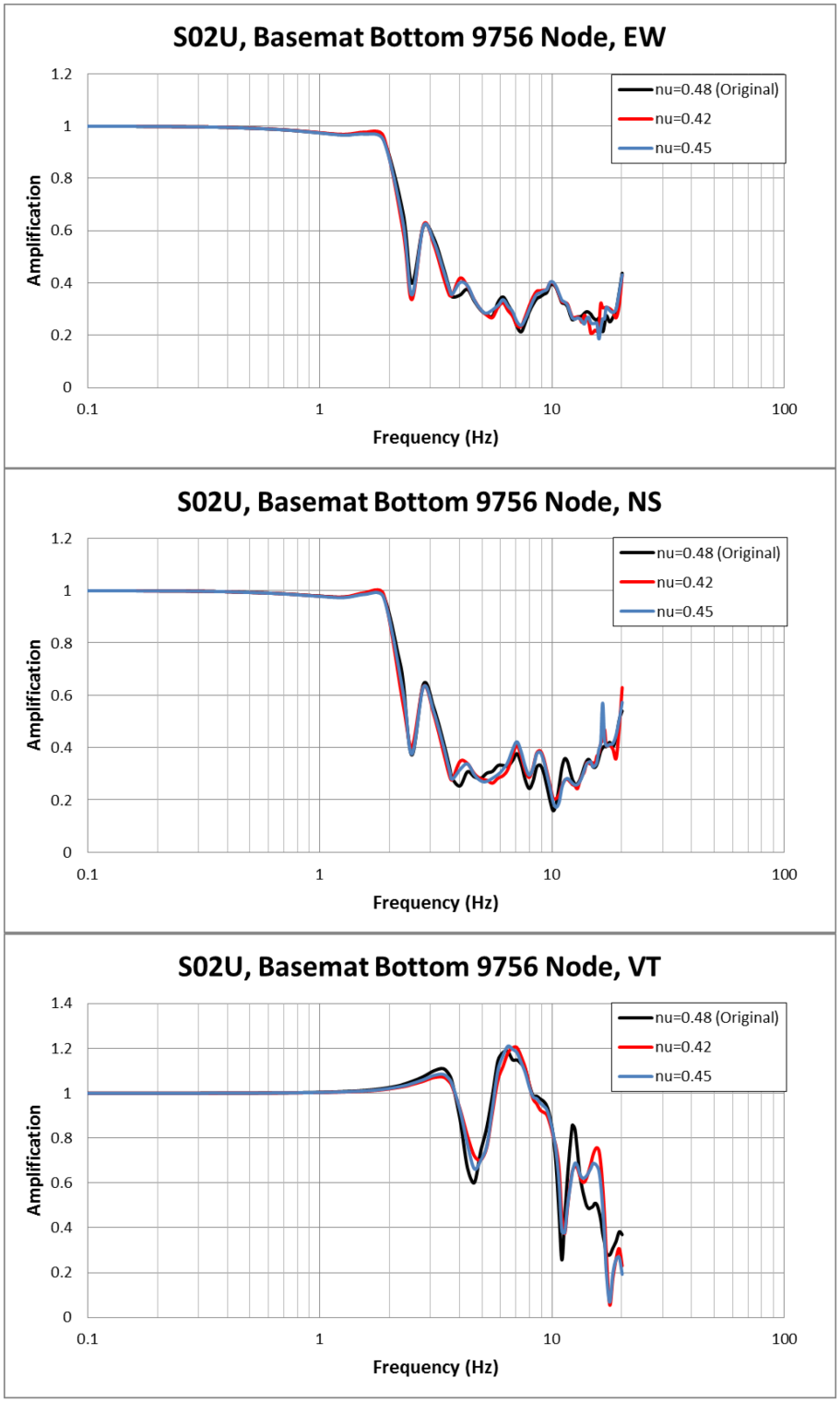

Figure 41. Comparison of Transfer Functions of 9756 Node at Basemat Bottom Elevation (S2 Soil Profile, Uncracked Concrete Stiffness Case)

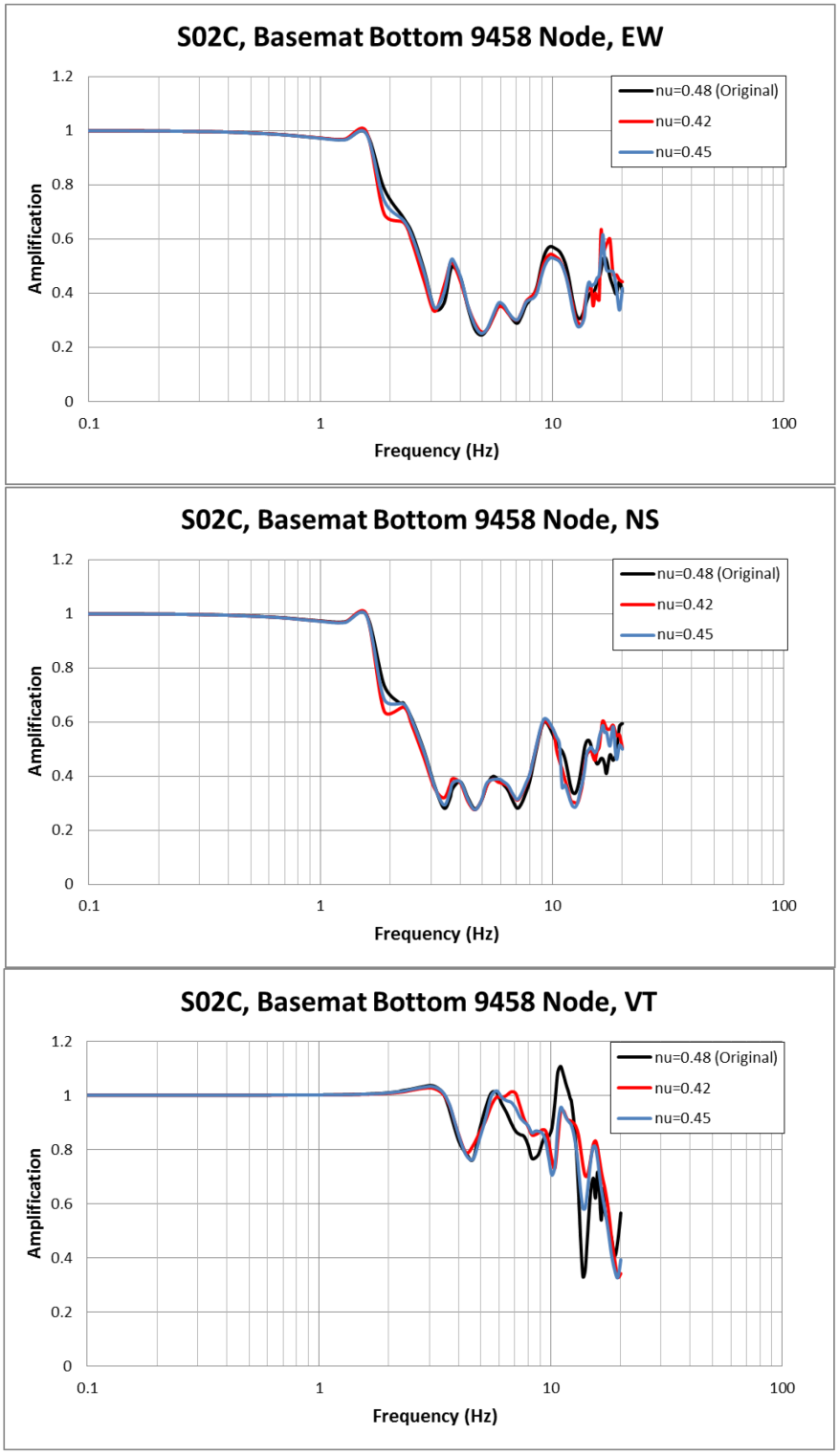

Figure 42. Comparison of Transfer Functions of 9458 Node at Basemat Bottom Elevation (S2 Soil Profile, Cracked Concrete Stiffness Case)

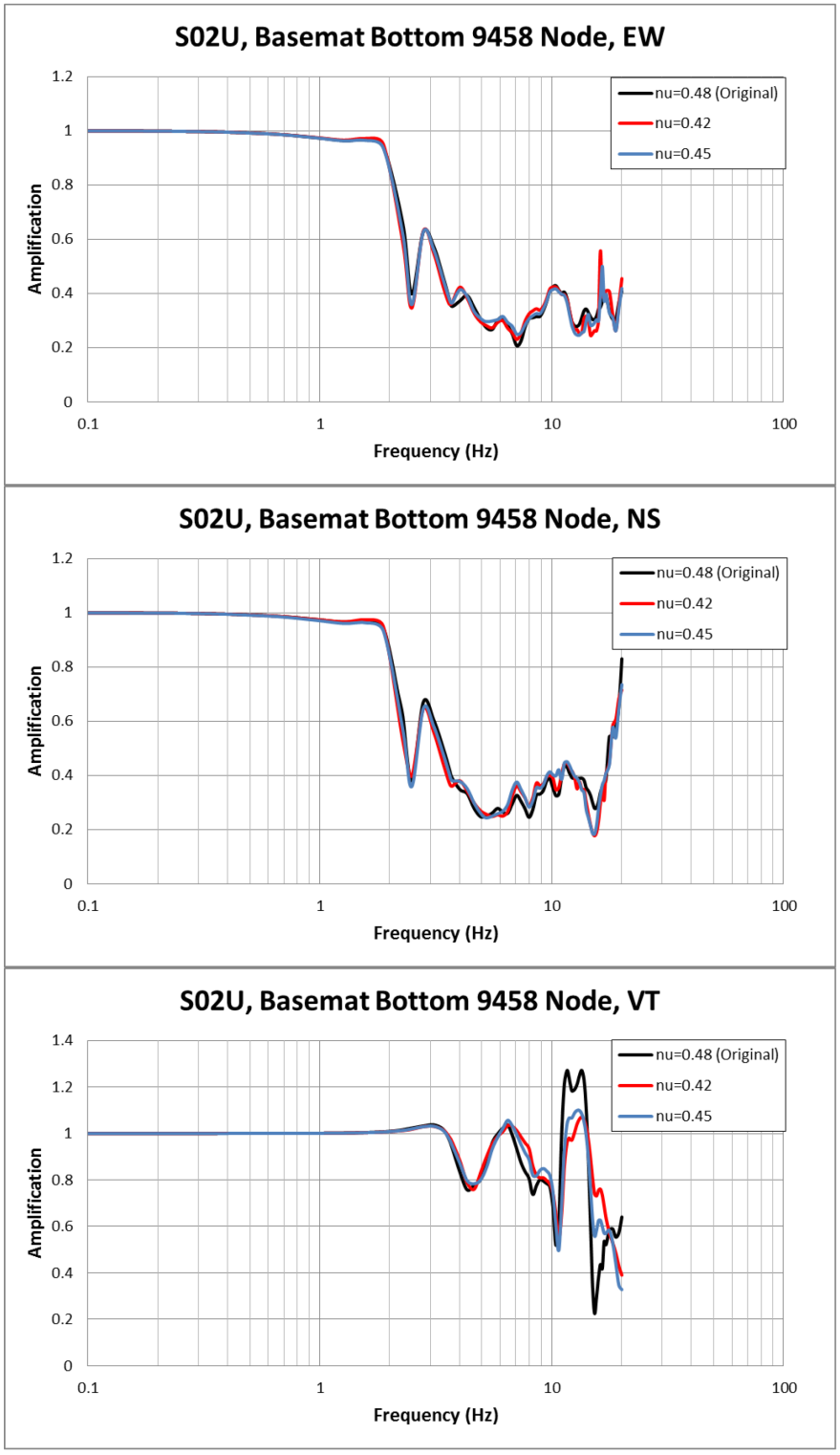

Figure 43. Comparison of Transfer Functions of 9458 Node at Basemat Bottom Elevation (S2 Soil Profile, Uncracked Concrete Stiffness Case)

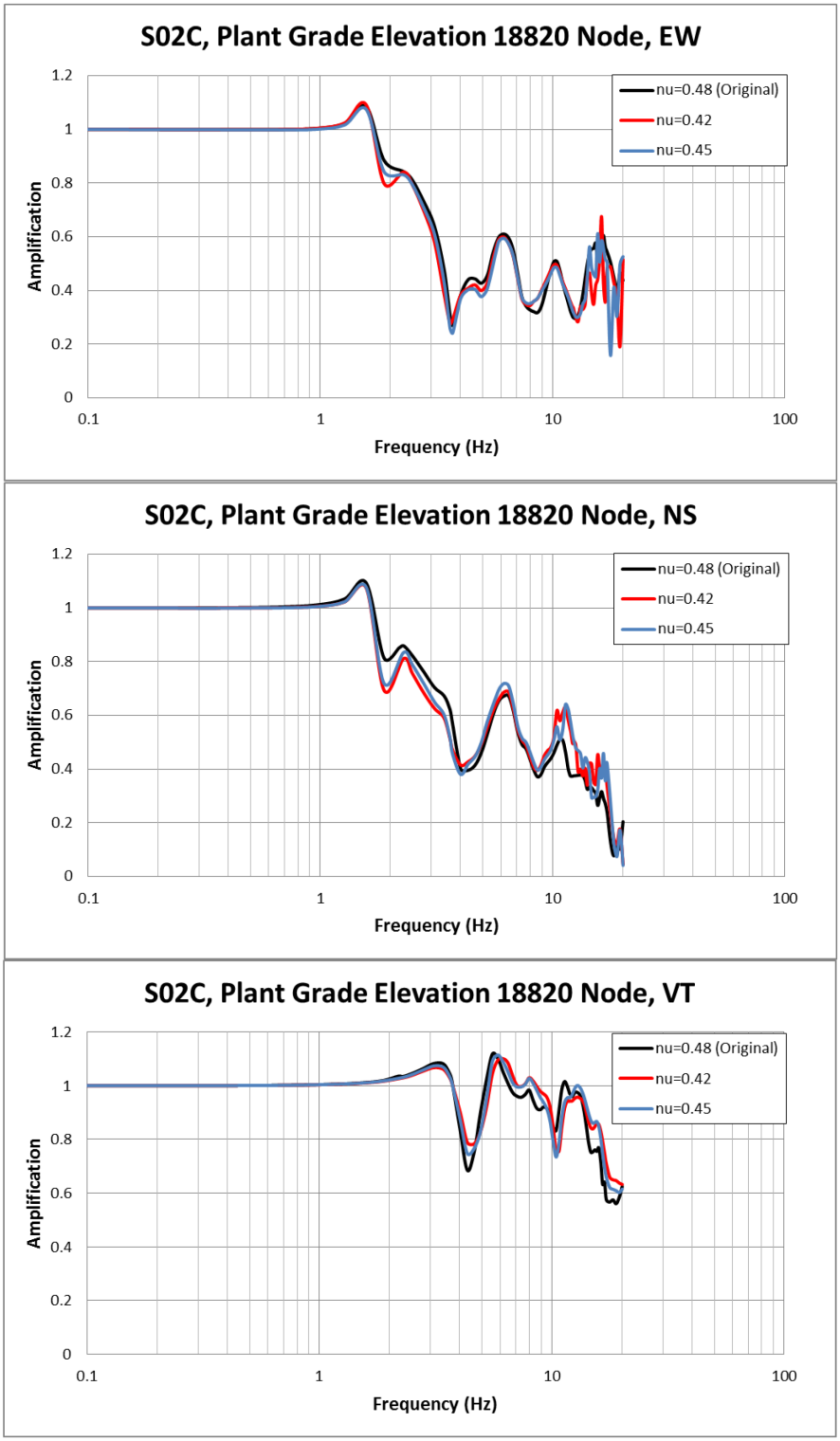

Figure 44. Comparison of Transfer Functions of 18820 Node at Plant Grade Elevation (S2 Soil Profile, Cracked Concrete Stiffness Case)

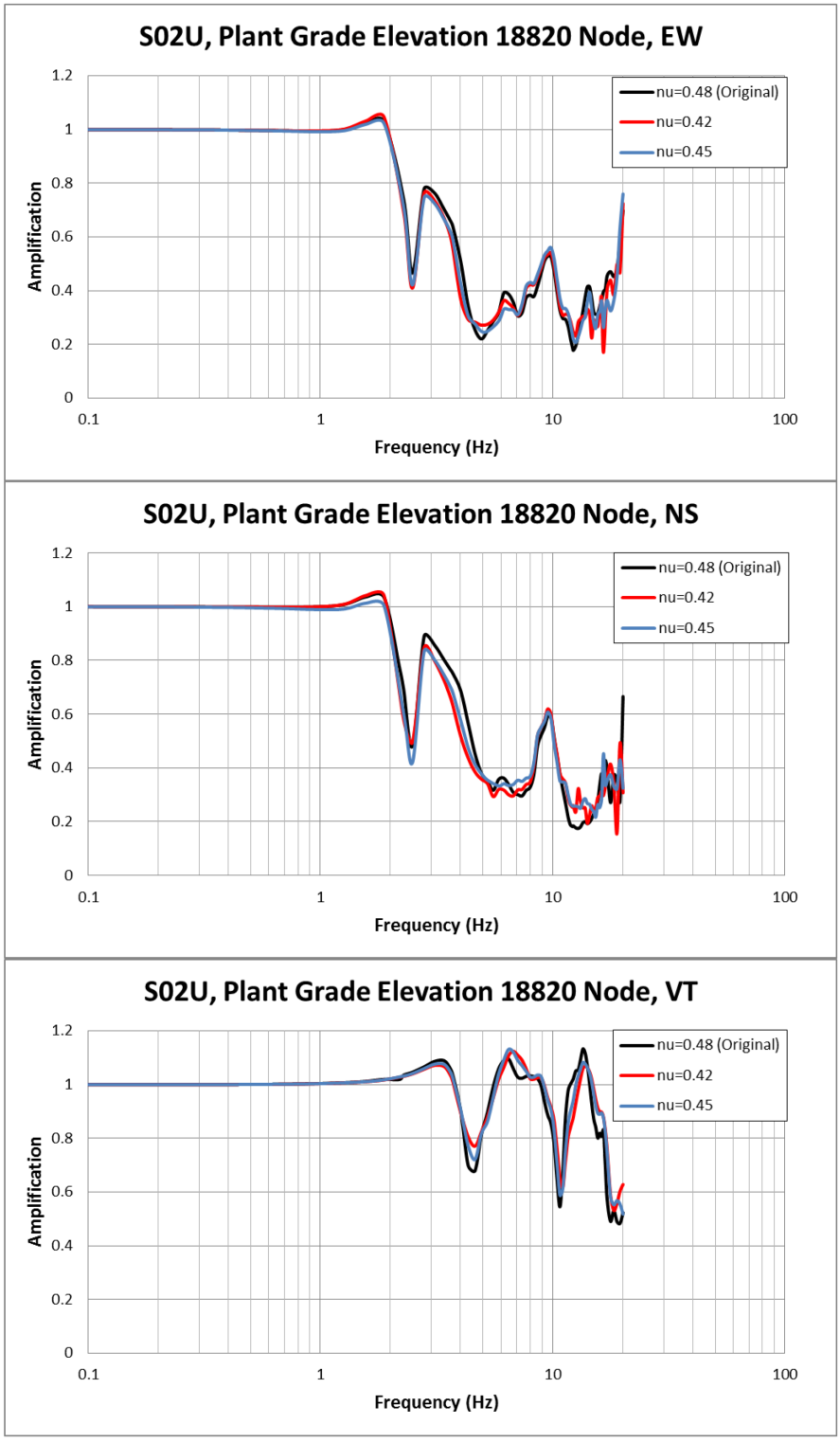

Figure 45. Comparison of Transfer Functions of 18820 Node at Plant Grade Elevation (S2 Soil Profile, Uncracked Concrete Stiffness Case)

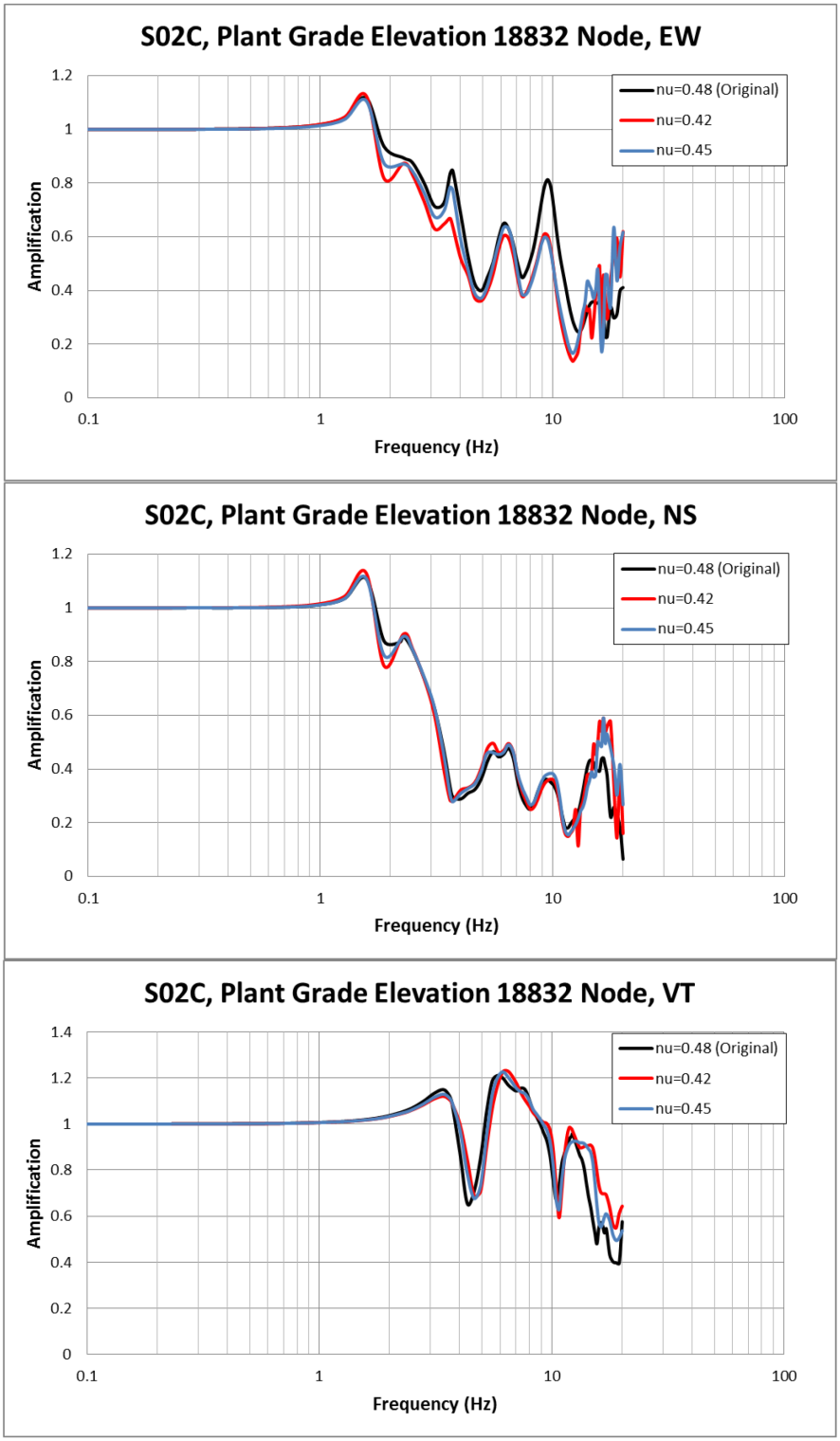

Figure 46. Comparison of Transfer Functions of 18832 Node at Plant Grade Elevation (S2 Soil Profile, Cracked Concrete Stiffness Case)

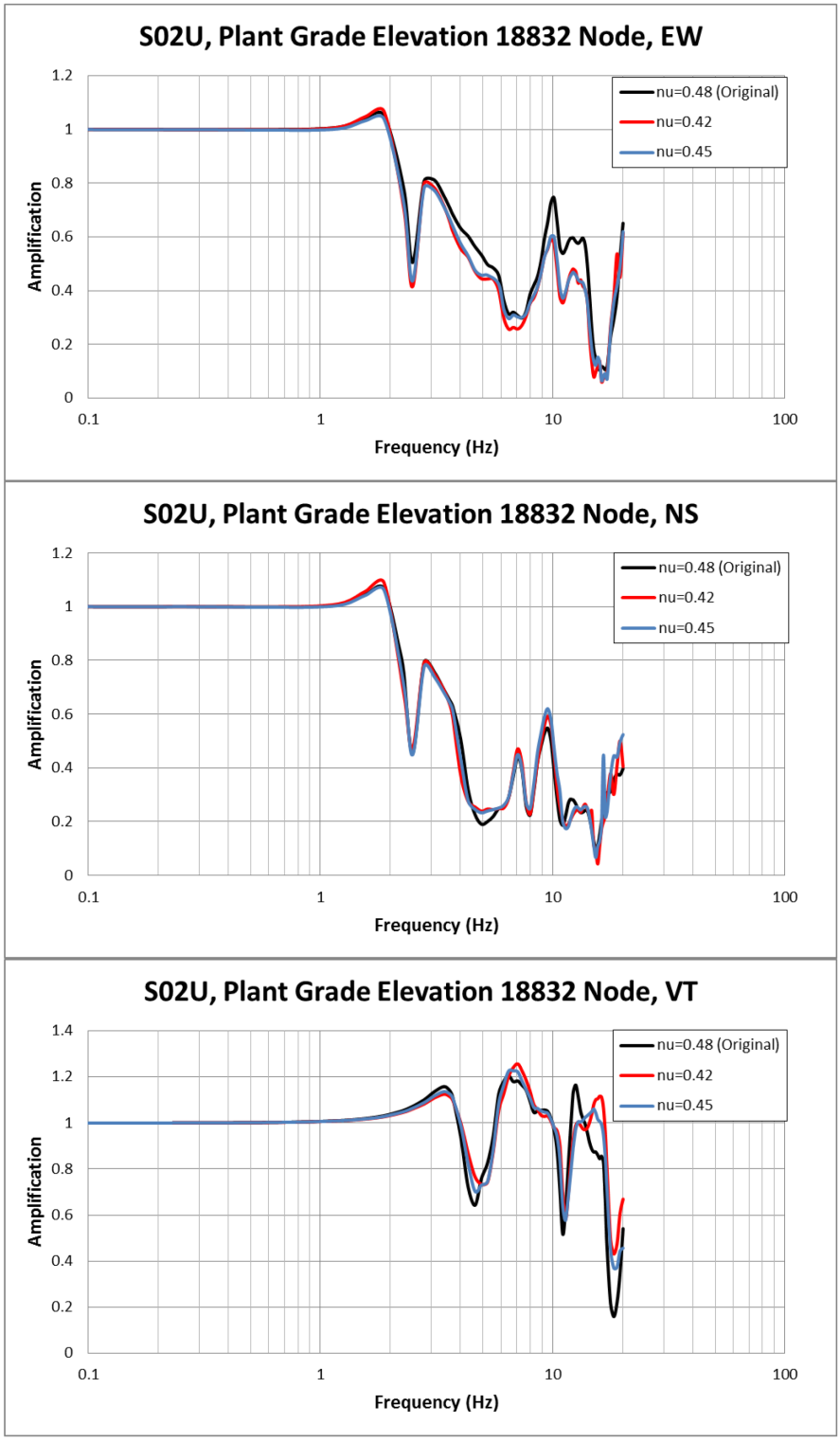

Figure 47. Comparison of Transfer Functions of 18832 Node at Plant Grade Elevation (S2 Soil Profile, Uncracked Concrete Stiffness Case)

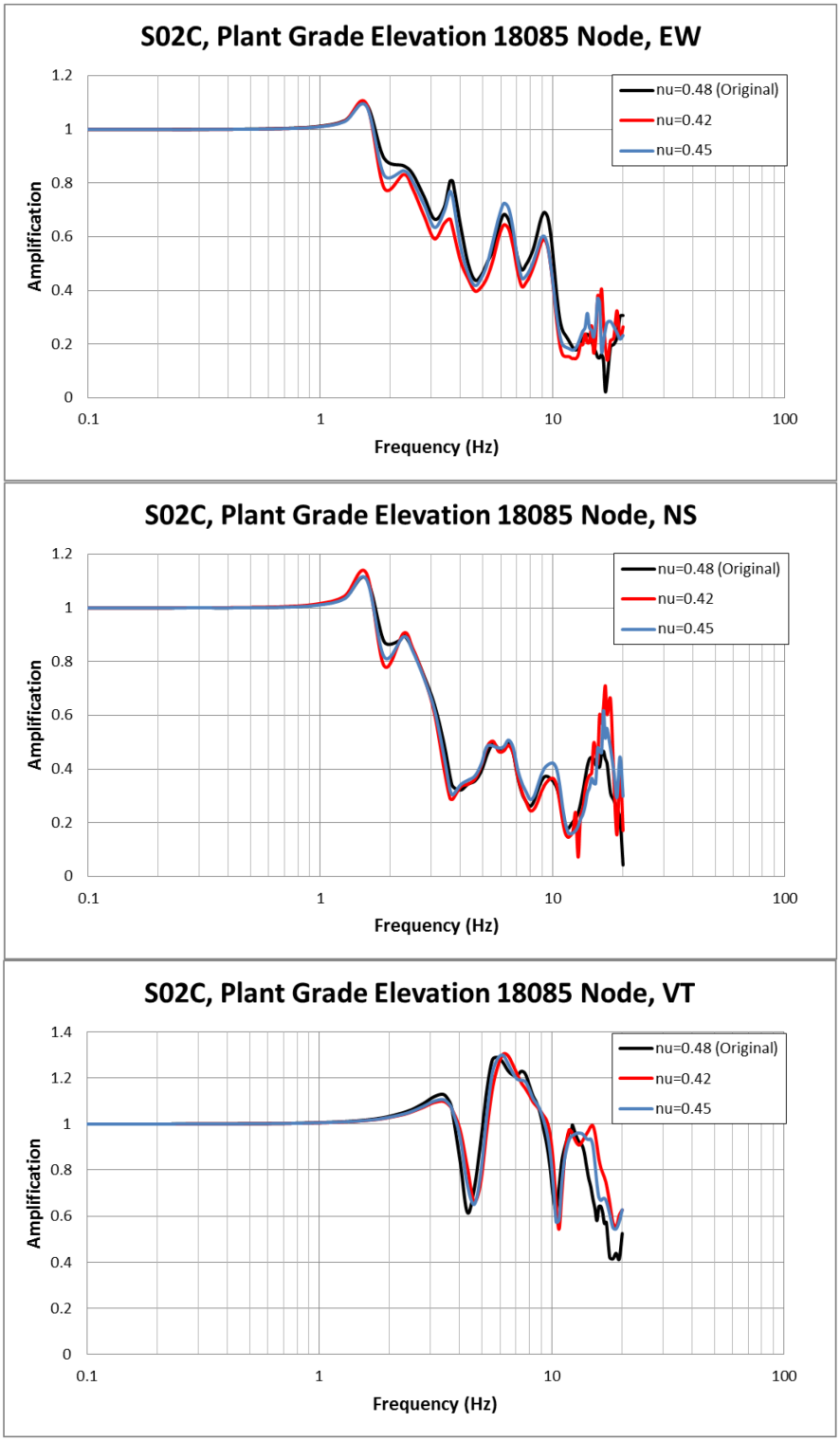

Figure 48. Comparison of Transfer Functions of 18085 Node at Plant Grade Elevation (S2 Soil Profile, Cracked Concrete Stiffness Case)

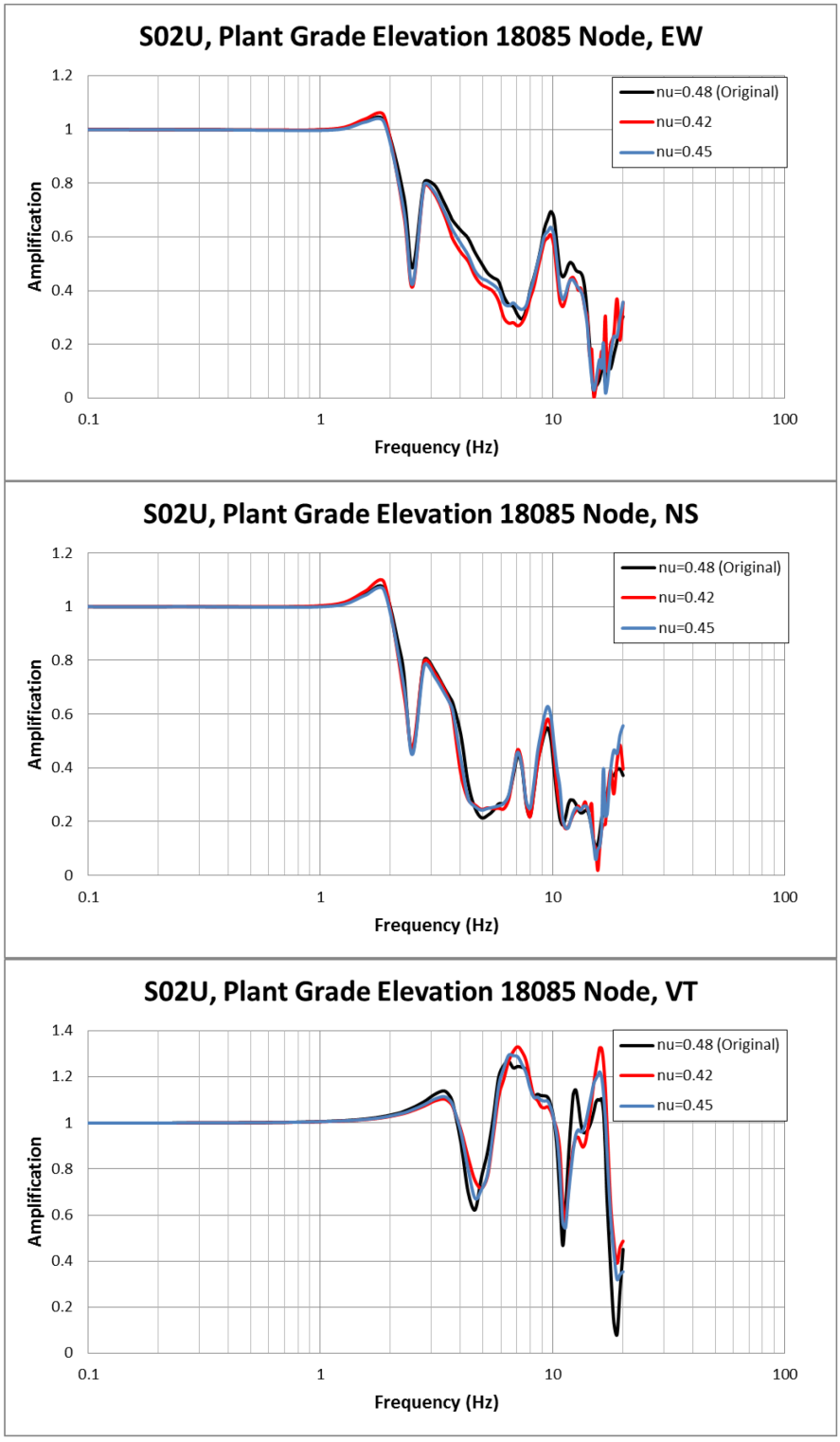

Figure 49. Comparison of Transfer Functions of 18085 Node at Plant Grade Elevation (S2 Soil Profile, Uncracked Concrete Stiffness Case)

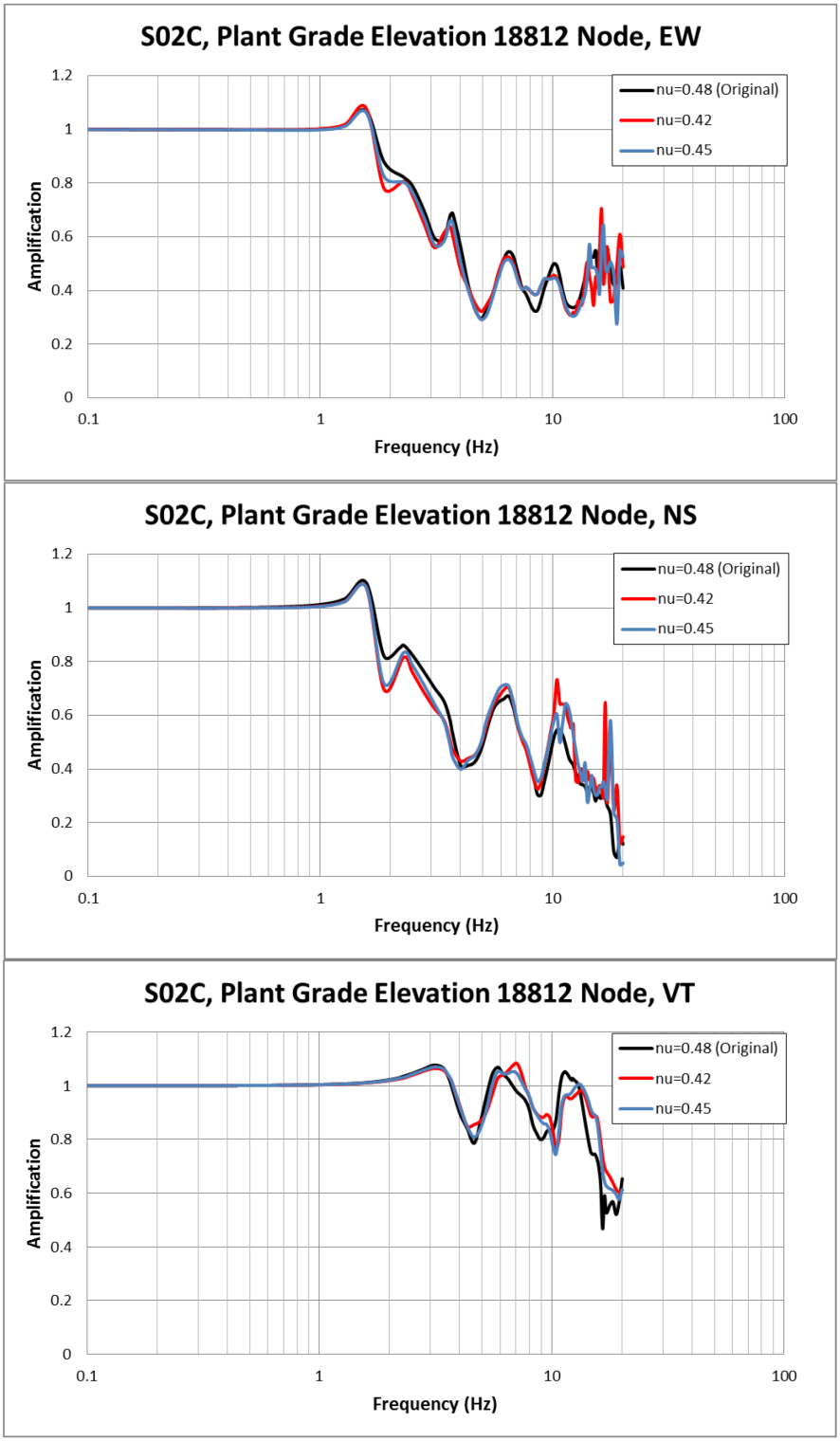

Figure 50. Comparison of Transfer Functions of 18812 Node at Plant Grade Elevation (S2 Soil Profile, Cracked Concrete Stiffness Case)

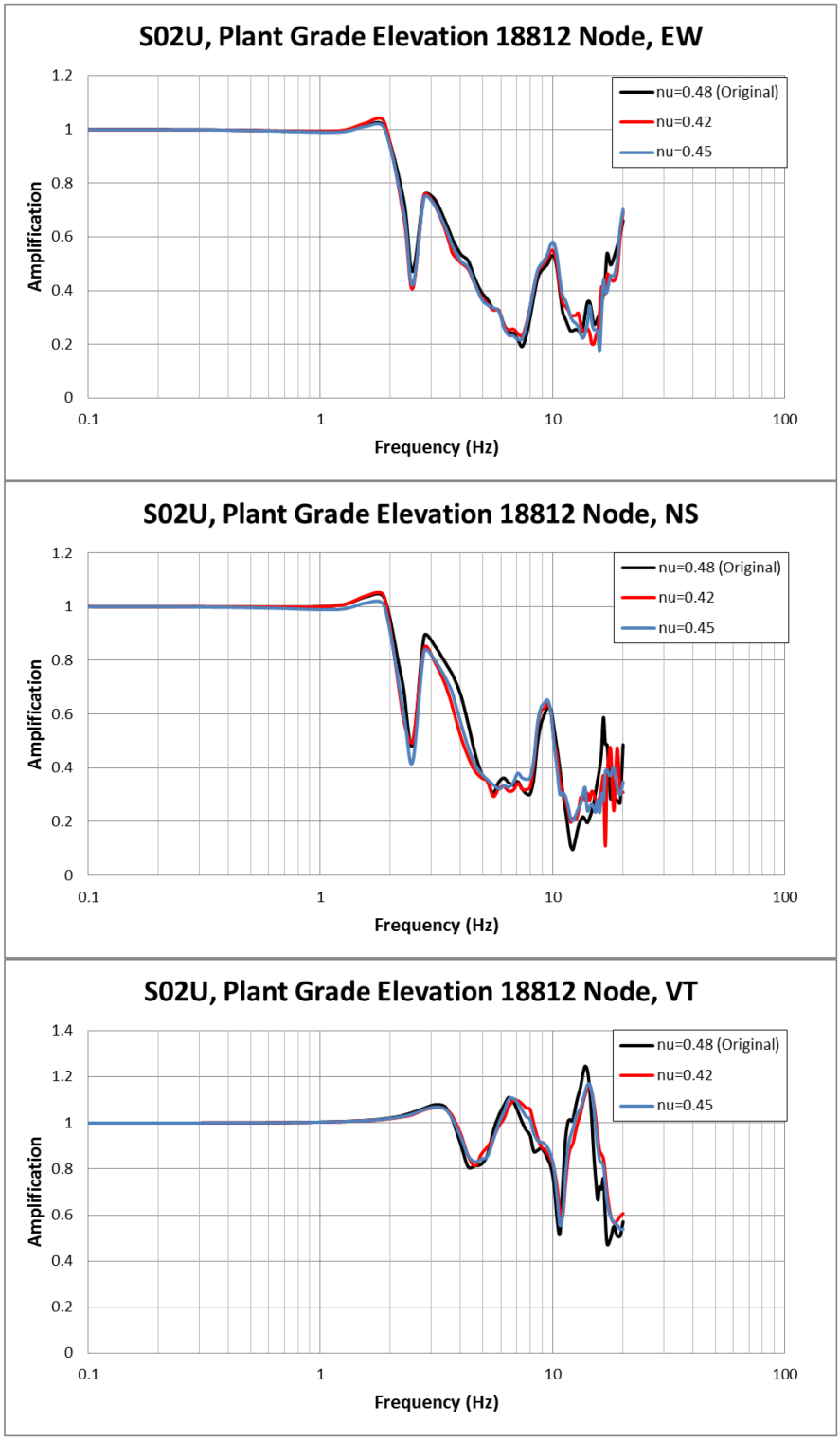

Figure 51. Comparison of Transfer Functions of 18812 Node at Plant Grade Elevation (S2 Soil Profile, Uncracked Concrete Stiffness Case)

Impact on DCD

DCD Tier 2, Subsection 3.7.2.3.3 will be revised, as indicated in Attachment 2 to this response.

Impact on PRA

There is no impact on the PRA.

Impact on Technical Specifications

There is no impact on the Technical Specifications.

Impact on Technical/Topical/Environmental Reports

Technical report APR1400-E-S-NR-14002-P/NP will be revised, as indicated in Attachments 1, 2, and 3 to this response.

RAI 252-8299 - Question 03.07.02-7

2 METHODOLOGY OF FEM DEVELOPMENT FOR NI STRUCTURES

The following considerations are made in the FEM development for the APR1400 NI structures:

- The APR1400 NI structures have a maximum embedded ratio (embedment depth/AB building height=55/171.8) of 0.320 and are considered embedded structures for the seismic SSI analysis.
- Estimates of the maximum frequencies of seismic wave propagation for the nine (9) soil profiles defined in the APR1400 are shown in Table 2-1 for soil layers that are 11 ft thick in the embedment. Among the nine (9) soil cases, five (5) have a maximum frequency above 50 Hz. A soil layer thickness of 11 ft is considered adequate and is accordingly adopted as the mesh size for soil elements and for the NI structural FEM.
- The 10 ft basemat is modeled by shell elements at the bottom surface of the basemat, rather than at the middle surface. This consideration can be justified as the SSI effects are accounted for more closely.
- The effects of vertical shear deformation in a 10-ft-thick common basemat on the seismic SSI analysis are considered insignificant.
- The effects of stiffnesses of local walls (not designed for the shear wall system) on the SSI response are considered small and are not included in the model.

The purpose of the model development is to create a 3-D FEM for SSI analysis of the APR1400 NI structures, which includes the RCB and AB founded on a common basemat. The 3-D SSI analysis is carried out using the SASSI program. The development of a complex 3-D finite element SASSI model of the NI structures consists of the following steps:

Insert "A" from page 2.

- A 3-D primitive model consisting of geometric properties of lines, areas, and volumes is created using the ANSYS program and based on data from the APR1400 drawings. The ANSYS primitive model consists of lines for columns and beams, areas for walls and slabs, and volumes for solid structural components, using key points to define key locations of physical wall-slab connection joints. In the primitive model, all material and geometrical properties are prepared.
- Based on the ANSYS primitive model, fine and coarse models are generated with specified element types, properties, and required mesh sizes.
- The ANSYS coarse model is validated by constructing an ANSYS fine model, obtaining analysis results, and comparing the results to the analysis results of the ANSYS coarse model.
- When the ANSYS AB and RCB coarse models have been verified, the primitive models are combined to create an ANSYS coarse 3-D FEM of the NI structures.
- The ANSYS coarse 3-D FEM of NI structures is converted to SASSI for a 3-D SSI analysis of NI structures.
- The SASSI 3-D FEM of NI structures is numerically optimized for efficient SSI computation.
- The SASSI 3-D FEM of NI structures is verified with its seismic response time histories obtained from the fixed-base condition against those obtained from the ANSYS coarse fixed-base 3-D FEMs of the AB and RCB. The SASSI 3-D FEM of NI structures can be verified by comparing the in-structure response spectra (ISRS) at selected locations.

Deleted

"A"

- The ANSYS fine-mesh and coarse-mesh FEMs for the fixed-base RCB and the AB are first developed and analyzed with the fixed-base condition to (1) generate 1-g lateral static-load response displacements, (2) extract fixed-base dynamic modal properties (natural frequencies and associated mode shapes and participation factors, and (3) develop fixed-base, 5%-damped in-structure response spectra (ISRS) at selected sufficiently representative structure locations. The ANSYS coarse-mesh models are verified against their corresponding ANSYS fine-mesh FE models to ensure that the model properties of the ANSYS coarse-mesh models are dynamically adequate as compared to the ANSYS fine-mesh FE models.

- When the ANSYS coarse-mesh models of the RCB and the AB are verified, the two models are combined to create an ANSYS coarse-mesh FE model of the NI structures.

- The fixed-base ANSYS coarse-mesh FE model of the NI structures is converted to the fixed-base SASSI structure model using the ACS SASSI model translator. The converted SASSI structure model is checked manually to ensure that the SASSI structure model is appropriately converted from the ANSYS model.

- The converted SASSI fixed-base structure model is analyzed for the fixed-base condition to develop fixed-base seismic acceleration response transfer functions and the corresponding 5%-damped ISRS at the same selected representative structure locations as those selected for the ANSYS model. These ISRS results are compared with the corresponding results obtained from the fixed-base ANSYS structure model to verify that the converted fixed-base SASSI structure model produces results which are sufficiently similar to the corresponding results of the fixed-base ANSYS structure model.

- The SASSI foundation model which is combined with the SASSI structure model consists of a common basemat structure model, an excavated soil volume model for the structure embedment developed to use the SASSI Direct Method (DM), and a backfill soil model, which is treated as a part of the structure model. The SASSI foundation model for the NI structures is so developed and checked manually.

- The common basemat for the AB and the RCB is modeled separately by 4-node shell elements for the AB at the bottom surface of concrete foundation (El. 45'-0") to specially account more closely for the soil-structure interaction effects, and by 8-node solid elements for the RCB concrete foundation. To ensure continuity of rotational deformation at the interface of the AB shell elements and the RCB solid elements, a dummy massless ring of shell elements is extended from the outside edge to the inside of RCB, beneath the solid elements. To simulate the relatively rigid 10-ft basemat between the top (El. 55'-0") and the bottom (El. 45'-0") surfaces of the concrete foundation for the AB, the AB walls and columns are extended from El. 55'-0" to El. 45'-0" with massless rigid beam elements.

- The ability of the resulting SASSI FE SSI model to translate and rotate is demonstrated by observing that the resulting seismic response transfer functions are able to translate and rotate as a rigid body on the supporting soil.

c. Reinforced concrete emergency diesel generator building

3.7.2.3.2 Decoupling Criteria for Subsystems

As recommended in the SRP 3.7.2 (Reference 16), the following decoupling criteria are used when a subsystem needs to be modeled:

a. If $R_m < 0.01$, decoupling is performed for any R_f

b. If $0.01 < R_m < 0.1$, decoupling is performed if $R_f \leq 0.8$ or $R_f \geq 1.25$

c. If $R_m > 0.1$, an approximate dynamic model of the subsystem is included in the main structural system

Where:

$$R_m = \frac{\text{total mass of the supported subsystem}}{\text{total mass of the supporting system}}$$

$$R_f = \frac{\text{fundamental frequency of the supported subsytem}}{\text{dominant frequency of the support motion}}$$

In general, most subsystems such as equipment and piping, with the exception of the reactor coolant system (RCS) and of the polar crane in reactor containment building, are decoupled from the floor that supports them.

3.7.2.3.3 Modeling of Safety-related Structures

Safety-related structures are modeled as three-dimensional FEMs. Major structural element systems such as floor slabs, foundation mat, roof slab, shear walls, and main frames are included in the FEM. All subsystems such as equipment and piping are considered in accordance with the decoupling criteria described in Subsection 3.7.2.3.2. For all seismic analyses, the dead load, live load, and attachment load to piping, cable tray and miscellaneous equipment mass are assumed to contribute to the inertial forces. In addition, mass associated with all heavy equipment is also included in the computation of floor or wall masses.

Insert "A" from page 2.

RAI 252-8299 - Question 03.07.02-7

RAI 252-8299 - Question 03.07.02-7 Rev.2

"A"

In general, in addition to the mass of the tributary structure dead load, additional mass equivalent to 25% of the specified floor live load or 75% of the specified snow load, where applicable; 2.394 kN/m^2 (50 psf), the equivalent of the miscellaneous dead load supported on the floors; and 0.479 kN/m^2 (10 psf), the equivalent of the attachment load on each face of the walls are included in the calculation of the inertia forces of the FEM.

seismic analysis model of the

Some exceptions are considered for floors in the reactor containment building and the roof of the auxiliary building. The seismic live load is not considered for floors in the reactor containment building. ~~The design floor live load inside the reactor containment building is generated by movable heavy equipment during construction and maintenance of the plant. During normal operation, the live load is negligible since equipment removal is not allowed in the reactor containment building.~~ The 2.394 kN/m^2 (50 psf) load equivalent to the roofing material dead load is only considered for the roof of the auxiliary building due to the containment dome not having roofing material.

because the effect of seismic live load on the reactor containment building seismic response has been shown by analysis to be negligibly small.

RAI 252-8299 - Question 03.07.02-7

LIST OF TABLES

Table 3-4 Seismic Live Load, Roof Snow Load, and Miscellaneous Dead Load

RAI 252-8299 - Question 03.07.02-7

applied on the roof. This criterion is applied to the CS dome. The mass of major equipment is distributed over specific tributary areas where applicable.

The applied loads from which masses are derived for the RCB are:

- Structure Self Weight

  The seismic live load, roof snow load, and miscellaneous dead load applied to slabs and dome of the RCB are presented in Table 3-4.

  Table 3-2 shows the mass densities used to represent the self weight of the RCB. Additional mass density is added to the CS shell density to account for a 0.25 in. steel liner plate that is compositely attached to the interior face of the CS cylinder and dome. To account for miscellaneous loads such as pipes, tank water and steel liner plates, an additional load of 10 psf is added to exterior walls, and 20 psf is added to all interior walls.

- Polar Crane Loads

  The polar crane load including the main girders (bridge), polar crane ring, trolley, rail, and accessories is approximately 2,500 kips. In addition, the polar crane attachment to the CS by means of steel brackets and steel ring beam weigh 500 kips. In summary, the total weight of the polar crane and its supporting system is approximately 3,000 kips. The polar crane is parked at azimuth 243°.

- Water Mass Loads

  The IRWST water mass is approximately 5,530 kips and is included in the FEM.

- Pipe Loads

  A 50 psf distributed dead load is applied on all RCB slabs to account for pipe loads attached to floor slabs, satisfying the NRC SRP 3.7.2, Part II, 3(D), of the acceptance criteria.

- Reactor Coolant System (RCS) Weights

  The self weight of the RCS supported at various elevations of the RCB is approximately 9,073 kips. This consists of various equipments and their attachments, components such as pipes, pumps, pressurizer, and steam generators.

- Roof or Snow Loads

  The controlling live load on the dome is 75% of 75 psf of snow loads. This load is applied as distributed to the dome (roof) of the CS according to the NRC SRP 3.7.2, Part II, 3(D), in the SRP acceptance criteria.

3.2.6 Modeling of Damping

For conservatism, operating basis earthquake (OBE) damping value of 4% for reinforced concrete and 3% for pre-stressed concrete and welded or bolted steel with friction connections are taken for the uncracked concrete case.

For the cracked concrete case, safe shutdown earthquake (SSE) damping values of 7% for cracked reinforced concrete and 4% for steel connections, as well as 5% for pre-stressed concrete, are used. This criterion is in compliance with NRC Regulatory Guide (RG) 1.61 (Reference 7). A low critical damping ratio of 0.5% is used for sloshing of water per the ASCE 4-98 requirement (Reference 8).

RAI 252-8299 - Question 03.07.02-7

3.2.7 Modeling of Hydrodynamic Effects for the IRWST

The hydrodynamic effect of significant mass interacting with the structure is considered for the IRWST in modeling the inertial characteristics in accordance with Subsection 4.5.4 in the APR1400 design criteria. Convective and impulsive horizontal masses and frequencies are calculated for modeling the hydrodynamic effects on tank walls.

- IRWST Description

  The IRWST is an enclosed annular cylindrical water tank located inside the RCB at El. 81'-0". Figure 3-8 is an elevation view of the tank, and Figure 3-9 is a plan view of the tank. The tank is made of reinforced concrete and consists of the roof slab, outer (exterior) wall, inner (interior) wall, and bottom slab, which rests on top of the RCB basemat. The inner radius of the outer wall is 71.83 ft, and the outer radius of the inner wall is 53 ft. The top elevation of the IRWST roof slab is 100'-0" and the top elevation of the bottom slab is 81'-0". The outer and inner walls, roof slab, and bottom slab are all 3 ft thick. The water at the normal operating level is at El. 93'-0". Thus, the water height from the top of the bottom slab to the bottom of the roof slab during normal operation is 12 ft, and the freeboard (water surface to the bottom of the roof slab) is 4 ft.

- Hydrodynamic Analytical Approach

  The analytical approach used to model the horizontal hydrodynamic effect on the annular cylindrical tank is based on the formulations given by Tang et al. (Reference 9), which are based on the previous study of dynamic responses of an annular cylindrical tank under horizontal seismic motion by Aslam et al. (Reference 10). This approach is also presented by R. A. Ibrahim.

  The hydrodynamic effects on the rigid tank in the formulation in Reference 9 can be simplified to equivalent mechanical models consisting of impulsive and convective parts similar to those formulated by Housner for cylindrical and rectangular tanks. The impulsive part represents a certain portion of water that moves as a rigid body with the bottom and walls. The convective part represents an oscillating (sloshing) portion of a certain portion of water responding as if it is an oscillating mass flexibly connected to the walls. Using the formulation given in Reference 9, the hydrodynamic properties of equivalent IRWST mechanical models, such as impulsive mass for the impulsive part, and sloshing frequencies and masses for the convective part, can be calculated.

  For the vertical vibration, all of the water in the tank is assumed to move vertically as a rigid body with the vertical motion of the tank base. Thus, all of the vertical water mass in the tank is uniformly distributed as lumped masses attached to structural nodes at the bottom of the tank.

- Summary of IRWST Hydrodynamic Properties

  The hydrodynamic properties for impulsive and convective parts are summarized in Table 3-4. In this table, the masses, frequencies, and axial spring stiffnesses of equivalent mechanical models are listed for the impulsive part, and the first two dominant sloshing modes for the convective parts.

3-5

The hydrodynamic effects of impulsive and convective parts of water contained in the IRWST are modeled separately by FEM using simplified mechanical models as described below.

RAI 252-8299 - Question 03.07.02-7

- Impulsive IRWST Models

  In order to simulate the impulsive forces to exert forces normal to the tank walls during horizontal seismic motion, the horizontal impulsive part of water, which represents the rigid portion of water mass moving with the tank, is modeled as a rigid circular ring-lumped mass, axially rigid radial beams (trusses) system, as shown in Figure 3-10. The impulsive mass given in Table 3-4 is uniformly distributed as lumped masses connected on a rigid circular ring. Each mass has two dynamic degrees of freedoms (DOFs) acting in the horizontal global X and Y directions and is equal to the impulsive mass given in Table 3-4 divided by the number of nodes on the ring.

  The rigid circular ring is made of inter-connected rigid beam with large axial and flexural properties to ensure that all impulsive masses move together as one system. The rigid ring is connected to axially flexible radial beams, which are connected to structural nodes on the FEM of the inner-tank wall. The radial beams have a large axial property and very small shear and flexural properties to simulate truss elements so the impulsive forces exert normal to the tank wall.

  3-5

  For the vertical vibration, all of the water in the tank is assumed to move vertically as a rigid body with the vertical motion of the tank base. Thus, the vertical impulsive model consists of lumping all of the water mass attached to FEM structural nodes at the tank base, as shown in Figure 3-12. Each lumped mass has only one dynamic DOF in the vertical global Z direction, and is equal to the total water mass contained in the tank divided by the number of structural nodes at the tank base.

- Convective IRWST Models

  In order to simulate water loads acting normal to the tank wall, the first two dominant modes of vibration of the convective part of the water in the tank, which represent the oscillating portion of water in the tank, are modeled by two lumped mass radial beam systems, as shown in Figure 3-11. The lumped masses for the first and second modes given in Table 3-4 are placed at the center of the tank. Each lumped mass is then connected to 41 axially flexible radial beams, which are connected to structural nodes on the FEM of the inner tank wall. The water damping ratio of 0.5% for horizontal sloshing modes, as required by ASCE 4-98, “Seismic Analysis and Safety-Related Nuclear Structures and Commentary,” is used as the damping value for radial beams in the ANSYS FEM.

3.2.8 Modeling of Polar Crane

The polar crane is modeled in the FEM. The polar crane is a standard two-girder overhead crane with end trucks at the girder centerlines. The crane is supported by the CS cylindrical shell at El. 241’-0”. Figure 3-13 shows the details of modeling the polar crane in the ANSYS.

The polar crane system is modeled at its parked location at azimuth 243°. The trolley masses and upper platform are modeled at the bridge girders in the second quarter of span location.

The polar crane model consists of the following:

- Two main steel girders are modeled to represent the bridge beams and support the trolley. The bridge wheels have been also modeled to represent the bridge width using rigid beams at all four (4) corners.

- The trolley is not modeled. The trolley structure is rigid and spans the two (2) main girders. It is idealized at its parked location by means of two (2) rigid mass less steel cross beams spanning the main girders forming the trolley frame. The trolley mass is accounted for as lumped mass.

RAI 252-8299 - Question 03.07.02-7

RAI 252-8299 - Question 03.07.02-7_Rev.2

Table 3-4

Seismic Live Load, Roof Snow Load, and Miscellaneous Dead Load

Floor Loads	Value (psf)
Miscellaneous dead load (minor equipment, piping, raceways, NRC SRP 3.7.2)	50.00
Seismic live load[1)] (25% of floor design load 200 psf, NRC SRP 3.7.2)	Not Applied
Roof snow load (75% of roof design snow load 75 psf, NRC SRP 3.7.2)	56.25

Notes

1) ~~The design floor live load inside the RCB is generated by movable heavy equipment during construction and maintenance of the plant. During normal operation, the live load is negligible since equipment removal is not allowed in the RCB. Also, the seismic load is considered not to occur during the construction and maintenance of the plant. Therefore, the seismic inertial floor live load is not applied to the seismic analysis of the RCB.~~

Table is added.

The seismic live load is not considered for floors in the seismic analysis model of the RCB because the effect of seismic live load on the RCB seismic response has been shown by analysis to be negligibly small.

RAI 252-8299 - Question 03.07.02-7

Table ~~3-4~~ 3-5

Hydrodynamic Properties for Equivalent Mechanic Models In-containment Refueling Water Storage Tank

Hydrodynamic Component	Mode	Kn[1]	Mn[2]	Wn[3]	ωn[4]	fn[5]	hn[6]
	n[7]	(lb/ft)	(lb-sec^2/ft)	(lb)	(rad/sec)	(Hz)	(ft)
Impulsive	rigid	rigid	5.769E+04	1.858E+06	very high	very high	5.2
Convective (Sloshing)	1	8,569	8.664E+04	2.790E+06	0.31	0.050	6.0
	2	144,500	2.647E+04	8.523E+05	2.34	0.372	7.5

Notes

1) Kn = Axial spring stiffness for mode n
2) Mn = Hydrodynamic mass for mode n
3) Wn = Hydrodynamic weight for mode n
4) ωn = Sloshing frequency in radian/second for mode n
5) fn = Sloshing frequency in Hertz (Hz) or cycle/second (cps) for mode n
6) hn = Height of impulsive or sloshing mass (Mn) from the bottom of the tank at El. 81'-0" for mode n
7) n = Mode number

RAI 252-8299 - Question 03.07.02-7

TABLE OF CONTENTS

RAI 252-8299 - Question 03.07.02-7

LIST OF FIGURES

RAI 252-8299 - Question 03.07.02-7

elements of the base. Mass duplication is avoided by assigning zero density to the penetrating shell elements.

3.2.13

~~3.2.12~~ Mesh Sizes for Generation of ANSYS Fine and Coarse 3-D FEM of RCB

The 3-D FE models have an adequate number of discrete mass degrees of freedom to capture the global and local translational, rocking, and torsional responses of the structures. The element size is selected so that the structural response is not significantly affected by further size refinement. In general, the fine model mesh size for the CS is 5 ft and for the IS approximately 6 ft. In contrast, the coarse mesh model element size is twice the fine mesh element sizes (i.e., 10 ft to 12 ft).

3.2.12 Modeling of RCS Support

The degrees of freedom compatibility condition between the beam elements of the RCS and solid elements of the PSW and the SSW is satisfied by using rigid beam elements at the beam-to-wall support points covering the footprint of the RCS support brackets. The RCS supports are modeled as rigid beam elements and connected with other rigid beam elements in the solid elements which represent the PSW and the SSW. Figure 3-21 shows the connection between the RCS supports and the solid elements.

RAI 252-8299 - Question 03.07.02-7

Add Figure 3-21 to next page of Figure 3-20.

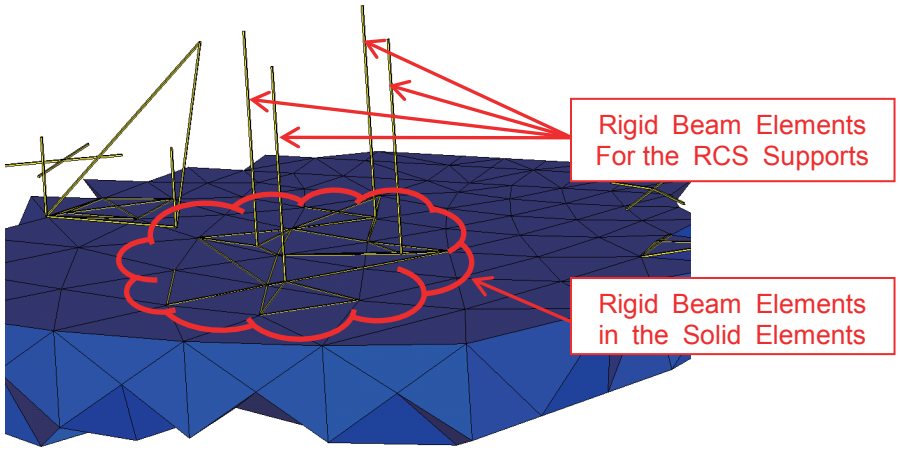

Figure 3-21 Connection between RCS Supports and Solid Elements